JL, Paul SM, Hawkins PN, Pham TH, Snyder C, Wesley RA, Hoffmann SC, Holland SM, Butman JA, Kastner DL: Neonatal-onset multisystem inflammatory disease responsive to interleukin-1beta inhibition. N Engl J Med. 2006; 355: 581-592.

44) Neven B, Prieur AM, Quartier dit Maire P; Medscape: Cryopyrinopathies: update on pathogenesis and treatment. Nat Clin Pract Rheumatol. 2008; 4: 481-489.

45) Feist E, Burmester GR: Canakinumab for treatment of cryopyrin-associated periodic syndrome. Expert Opin Biol Ther. 2010; 10: 1631-1636.

46) Toker O, Hashkes PJ: Critical appraisal of canakinumab in the treatment of adults and children with cryopyrin-associated periodic syndrome (CAPS). Biologics. 2010; 25: 131-138.

47) Houten SM, Kuis W, Duran M, de Koning TJ, van Royen-Kerkhof A, Romeijn GJ, et al: Mutations in MVK, encoding mevalonate kinase, cause hyperimmunoglobulinaemia D and periodic fever syndrome. Nat Genet. 1999; 22: 175-177.

48) Prieur AM: A recently recognised chronic inflammatory disease of early onset characterised by the triad of rash, central nervous system involvement and arthropathy. Clin Exp Rheumatol. 2001; 19: 103-106.

49) McTaggart SJ: Isoprenylated proteins. Cell Mol Life Sci. 2006; 63: 255-267.

50) Frenkel J, Rijkers GT, Mandey SH, Buurman SW, Houten SM, Wanders RJ, Waterham HR, Kuis W: Lack of isoprenoid products raises ex vivo interleukin-1beta secretion in hyperimmunoglobulinemia D and periodic fever syndrome. Arthritis Rheum. 2002; 46: 2794-2803.

51) Normand S, Massonnet B, Delwail A, Favot L, Cuisset L, Grateau G, Morel F, Silvain C, Lecron JC: Specific increase in caspase-1 activity and secretion of IL-1 family cytokines: a putative link between mevalonate kinase deficiency and inflammation. Eur Cytokine Netw. 2009; 20: 101-107.

52) Ammouri W, Cuisset L, Rouaghe S, Rolland MO, Delpech M, Grateau G, Ravet N: Diagnostic value of serum immunoglobulinaemia D level in patients with a clinical suspicion of hyper IgD syndrome. Rheumatology (Oxford). 2007; 46: 1597-1600.

53) Simon A, Drewe E, van der Meer JW, Powell RJ, Kelley RI, Stalenhoef AF, Drenth JP: Simvastatin treatment for inflammatory attacks of the hyperimmunoglobulinemia D and periodic fever syndrome. Clin Pharmacol Ther. 2004; 75: 476-483.

54) Bodar EJ, van der Hilst JC, Drenth JP, van der Meer JW, Simon A: Effect of etanercept and anakinra on inflammatory attacks in the hyper-IgD syndrome: introducing a vaccination provocation model. Neth J Med. 2005; 63: 260-264.

55) Nevyjel M, Pontillo A, Calligaris L, Tommasini A, D'Osualdo A, Waterham HR, Granzotto M, Crovella S, Barbi E, Ventura A: Diagnostics and therapeutic insights in a severe case of mevalonate kinase deficiency. Pediatrics. 2007; 119: e523-527.

56) Topaloglu R, Ayaz NA, Waterham HR, Yuce A, Gumruk F, Sanal O: Hyperimmunoglobulinemia D and periodic fever syndrome: treatment with etanercept and follow-up. Clin Rheumatol. 2008; 27: 1317-1320.

57) Neven B, Valayannopoulos V, Quartier P, Blanche S, Prieur AM, Debré M, Rolland MO, Rabier D, Cuisset L, Cavazzana-Calvo M, de Lonlay P, Fischer A: Allogeneic bone marrow transplantation in mevalonic aciduria. N Engl J Med. 2007; 356: 2700-2703.

58) Shoham NG, Centola M, Mansfield E, Hull KM, Wood G, Wise CA, Kastner DL: Pyrin binds the PSTPIP1/CD2BP1 protein, defining familial Mediterranean fever and PAPA syndrome as disorders in the same pathway. Proc Natl Acad Sci U S A. 2003; 100: 13501-13506.

59) Aksentijevich I, Masters SL, Ferguson PJ, Dancey P, Frenkel J, van Royen-Kerkhoff A, Laxer R, Tedgård U, Cowen EW, Pham TH, Booty M, Estes JD, Sandler NG, Plass N, Stone DL, Turner ML, Hill S, Butman JA, Schneider R, Babyn P, El-Shanti HI, Pope E, Barron K, Bing X, Laurence A, Lee CC, Chapelle D, Clarke GI, Ohson K, Nicholson M, Gadina M, Yang B, Korman BD, Gregersen PK, van Hagen PM, Hak AE, Huizing M, Rahman P, Douek DC, Remmers EF, Kastner DL, Goldbach-Mansky R: An autoinflammatory disease with deficiency of the interleukin-1-receptor antagonist. N Engl J Med. 2009; 360: 2426-2437.

60) Aksentijevich I, Nowak M, Mallah M, Chae JJ, Watford WT, Hofmann SR, Stein L, Russo R, Goldsmith D, Dent P, Rosenberg HF, Austin F, Remmers EF, Balow JE Jr, Rosenzweig S, Komarow H, Sho-

ham NG, Wood G, Jones J, Mangra N, Carrero H, Adams BS, Moore TL, Schikler K, Hoffman H, Lovell DJ, Lipnick R, Barron K, O'Shea JJ, Kastner DL, Goldbach-Mansky R: De novo CIAS1 mutations, cytokine activation, and evidence for genetic heterogeneity in patients with neonatal-onset multisystem inflammatory disease (NOMID): a new member of the expanding family of pyrin-associated autoinflammatory diseases. Arthritis Rheum. 2002; 46: 3340-3348.

61) Feldmann J, Prieur AM, Quartier P, Berquin P, Certain S, Cortis E, Teillac-Hamel D, Fischer A, de Saint Basile G: Chronic infantile neurological cutaneous and articular syndrome is caused by mutations in CIAS1, a gene highly expressed in polymorphonuclear cells and chondrocytes. Am J Hum Genet. 2002; 71: 198-203.

62) Neven B, Callebaut I, Prieur AM, Feldmann J, Bodemer C, Lepore L, Derfalvi B, Benjaponpitak S, Vesely R, Sauvain MJ, Oertle S, Allen R, Morgan G, Borkhardt A, Hill C, Gardner-Medwin J, Fischer A, de Saint Basile G: Molecular basis of the spectral expression of CIAS1 mutations associated with phagocytic cell-mediated autoinflammatory disorders CINCA/NOMID, MWS, and FCU. Blood. 2004; 103: 2809-2815.

63) Hoffman HM, Mueller JL, Broide DH, Wanderer AA, Kolodner RD: Mutation of a new gene encoding a putative pyrin-like protein causes familialcold autoinflammatory syndrome and Muckle-Wells syndrome. Nat Genet. 2001; 29: 301-305.

64) Aganna E, Martinon F, Hawkins PN, Ross JB, Swan DC, Booth DR, Lachmann HJ, Bybee A, Gaudet R, Woo P, Feighery C, Cotter FE, Thome M, Hitman GA, Tschopp J, McDermott MF: Association of mutations in the NALP3/CIAS1/PYPAF1 gene with a broad phenotype including recurrent fever, cold sensitivity, sensorineural deafness, and AA amyloidosis. Arthritis Rheum. 2002; 46: 2445-2452.

65) Dodé C, Le Dû N, Cuisset L, Letourneur F, Berthelot JM, Vaudour G, Meyrier A, Watts RA, Scott DG, Nicholls A, Granel B, Frances C, Garcier F, Edery P, Boulinguez S, Domergues JP, Delpech M, Grateau G: New mutations of CIAS1 that are responsible for Muckle-Wells syndrome and familial cold urticaria: a novel mutation underlies both syndromes. Am J Hum Genet. 2002; 70: 1498-1506.

66) Aróstegui JI, Aldea A, Modesto C, Rua MJ, Argüelles F, González-Enseñat MA, Ramos E, Rius J, Plaza S, Vives J, Yagüe J: Clinical and genetic heterogeneity among Spanish patients with recurrent autoinflammatory syndromes associated with the CIAS1/PYPAF1/NALP3 gene. Arthritis Rheum. 2004; 50: 4045-4050.

67) Goldbach-Mansky R, Dailey NJ, Canna SW, Gelabert A, Jones J, Rubin BI, Kim HJ, Brewer C, Zalewski C, Wiggs E, Hill S, Turner ML, Karp BI, Aksentijevich I, Pucino F, Penzak SR, Haverkamp MH, Stein L, Adams BS, Moore TL, Fuhlbrigge RC, Shaham B, Jarvis JN, O'Neil K, Vehe RK, Beitz LO, Gardner G, Hannan WP, Warren RW, Horn W, Cole JL, Paul SM, Hawkins PN, Pham TH, Snyder C, Wesley RA, Hoffmann SC, Holland SM, Butman JA, Kastner DL: Neonatal-onset multisystem inflammatory disease responsive to interleukin-1beta inhibition. N Engl J Med. 2006; 355: 581-592.

68) Aksentijevich I, Remmers EF, Goldbach-Mansky R, Reiff A, Kastner DL: Mutational analysis in neonatal-onset multisystem inflammatory disease: Comment on the articles by Frenkel et al and Saito et al. Arthritis Rheum. 2006; 54: 2703- 2704.

69) Youssoufian H, Pyeritz RE: Mechanisms and consequences of somatic mosaicism in humans. Nat Rev Genet. 2002; 3: 748-758.

70) Fujisawa A, Kambe N, Saito M, Nishikomori R, Tanizaki H, Kanazawa N, Adachi S, Heike T, Sagara J, Suda T, Nakahata T, Miyachi Y: Disease-associated mutations in CIAS1 induce cathepsin B-dependent rapid cell death of human THP-1 monocytic cells. Blood. 2007; 109: 2903-2911.

71) Saito M, Fujisawa A, Nishikomori R, Kambe N, Nakata-Hizume M, Yoshimoto M, Ohmori K, Okafuji I, Yoshioka T, Kusunoki T, Miyachi Y, Heike T, Nakahata T: Somatic mosaicism of CIAS1 in a patient with chronic infantile neurologic, cutaneous, articular syndrome. Arthritis Rheum. 2005; 52: 3579-3585.

72) Saito M, Nishikomori R, Kambe N, Fujisawa A, Tanizaki H, Takeichi K, Imagawa T, Iehara T, Takada H, Matsubayashi T, Tanaka H, Kawashima H, Kawakami K, Kagami S, Okafuji I, Yoshioka T, Adachi S, Heike T, Miyachi Y, Nakahata T: Disease-associated CIAS1 mutations induce monocyte death, revealing low-level mosaicism in mutation-negative cryopyrin-associated periodic syndrome patients. Blood. 2008; 111: 2132-2141.

A Novel Serum-Free Monolayer Culture for Orderly Hematopoietic Differentiation of Human Pluripotent Cells via Mesodermal Progenitors

Akira Niwa[1,2], Toshio Heike[2], Katsutsugu Umeda[2,4], Koichi Oshima[1], Itaru Kato[1,2], Hiromi Sakai[5], Hirofumi Suemori[3], Tatsutoshi Nakahata[1,2], Megumu K. Saito[1,2]*

1 Clinical Application Department, Center for iPS Cell Research and Application, Kyoto University, Kyoto, Japan, **2** Department of Pediatrics, Graduate School of Medicine, Kyoto University, Kyoto, Japan, **3** Laboratory of Embryonic Stem Cell Research, Stem Cell Research Center, Institute for Frontier Medical Sciences, Kyoto University, Kyoto, Japan, **4** Institute of Molecular Medicine, University of Texas Health Science Center, Houston, Texas, United States of America, **5** Waseda Bioscience Research Institute in Helios, Singapore

Abstract

Elucidating the *in vitro* differentiation of human embryonic stem (ES) and induced pluripotent stem (iPS) cells is important for understanding both normal and pathological hematopoietic development *in vivo*. For this purpose, a robust and simple hematopoietic differentiation system that can faithfully trace *in vivo* hematopoiesis is necessary. In this study, we established a novel serum-free monolayer culture that can trace the *in vivo* hematopoietic pathway from ES/iPS cells to functional definitive blood cells via mesodermal progenitors. Stepwise tuning of exogenous cytokine cocktails induced the hematopoietic mesodermal progenitors via primitive streak cells. These progenitors were then differentiated into various cell lineages depending on the hematopoietic cytokines present. Moreover, single cell deposition assay revealed that common bipotential hemoangiogenic progenitors were induced in our culture. Our system provides a new, robust, and simple method for investigating the mechanisms of mesodermal and hematopoietic differentiation.

Citation: Niwa A, Heike T, Umeda K, Oshima K, Kato I, et al. (2011) A Novel Serum-Free Monolayer Culture for Orderly Hematopoietic Differentiation of Human Pluripotent Cells via Mesodermal Progenitors. PLoS ONE 6(7): e22261. doi:10.1371/journal.pone.0022261

Editor: Dan Kaufman, University of Minnesota, United States of America

Received January 4, 2011; **Accepted** June 18, 2011; **Published** July 27, 2011

Funding: This work was supported by grants from the Ministry of Education, Culture, Sports, Science, and Technology of Japan (#22790979). The funders had no role in study design, data collection and analysis, decision to publish, or preparation of the manuscript.

Competing Interests: The authors have declared that no competing interests exist.

* E-mail: msaito@kuhp.kyoto-u.ac.jp

Introduction

Because of pluripotency and self-renewal, human embryonic stem (ES) cells and induced pluripotent stem (iPS) cells are potential cell sources for regenerative medicine and other clinical applications, such as cell therapies, drug screening, toxicology, and investigation of disease mechanisms [1,2,3]. iPS cells are reprogrammed somatic cells with ES cell-like characteristics that are generated by introducing certain combinations of genes, proteins, or small molecules into the original cells [4,5,6,7]. Patient-derived iPS cells have facilitated individualized regenerative medicine without immunological or ethical concerns. Moreover, patient- or disease-specific iPS cells are an important resource for unraveling human hematological disorders. However, for this purpose, a robust and simple hematopoietic differentiation system that can reliably mimic in vivo hematopoiesis is necessary.

Mesodermal and hematopoietic differentiation is a dynamic event associated with changes in both the location and phenotype of cells [8,9,10,11]. Some primitive streak (PS) cells appearing just after gastrulation form the mesoderm, and a subset of mesodermal cells differentiate into hematopoietic cell lineages [9,12,13,14,15,16]. Previous studies have accumulated evidence on these embryonic developmental pathways.

The leading methods of blood cell induction from ES/iPS cells employ 2 different systems: monolayer animal-derived stromal cell coculture and 3-dimensional embryoid body (EB) formation. Both methods can produce hematopoietic cells from mesodermal progenitors, and combinations of cytokines can control, to some extent, the specific lineage commitment [1,2,17,18,19,20,21,22,23,24,25,26,27,28]. In the former method, a previous study showed that OP9 stromal cells, which are derived from the bone marrow of osteopetrotic mice, augment the survival of human ES cell-derived hematopoietic progenitors [29]. However, as the stromal cell condition controls the robustness of the system, it can be relatively unstable. Furthermore, the induction of hematopoietic cells from human pluripotent cells on murine-derived cells is less efficient than that from mice cells.

In EB-based methods, hematopoietic cells emerge from specific areas positive for endothelial markers such as CD31 [30,31,32]. Through these methods, previous studies have generated a list of landmark genes for each developmental stage, such as *T* and *KDR* genes for the PS and mesodermal cells, respectively [12,16,17,18,25,28,33,34,35,36], and also have emphasized appropriate developmental conditions consisting of specific microenvironments, signal gradients, and cytokines given in suitable combinations with appropriate timing. For robust and reproducible specification to myelomonocytic lineages of cells, some recent studies have converted to serum-independent culture by using EB formation [37]. However, the difficulty in applying 3-dimensional location information inside EBs prevents substantial increases in

hematopoietic specification efficacy. Additionally, the sphere-like structure of the EB complicates tracking and determination of hematopoietic–stromal cell interactions.

To overcome these issues, we established a novel serum-free monolayer hematopoietic cell differentiation system from human ES and iPS cells. Although there are no reports describing the shift of human ES/iPS cells from primitive to definitive erythropoiesis in a monolayer xeno-cell-free condition, our system can trace the in vitro differentiation of human ES/iPS cells into multiple lineages of definitive blood cells, such as functional erythrocytes and neutrophils. Hematopoietic cells arise via an orderly developmental pathway that includes PS cells, mesoderm, and primitive hematopoiesis.

Materials and Methods

Maintenance of human ES/iPS cells in serum-free condition

Experiments were carried out with the human ES cell lines KhES-1 and KhES-3 (kindly provided by Norio Nakatsuji) and iPS cell lines 201B7 and 253G4 (kindly provided by Shinya Yamanaka). Stable derivatives of ES cells carrying the transgene for green fluorescent protein (GFP) after CAG promoter were also used [38,39]. The ES/iPS cells were maintained on a tissue culture dish (#353004; Becton-Dickinson, Franklin Lakes, NJ) coated with growth factor-reduced Matrigel (#354230; Becton-Dickinson) in mTeSR1 serum-free medium (#05850; STEMCELL Technologies, Vancouver, BC, Canada). The medium was replaced everyday. Passage was performed according to the manufacturer's protocol.

Differentiation of ES/iPS cells

First, undifferentiated ES/iPS cell colonies were prepared at the density of less than 5 colonies per well of a 6-well tissue culture plate (#353046; Becton-Dickinson). When individual colony grew up to approximately 500 μm in diameter, mTeSR1 maintenance medium was replaced by Stemline II serum-free medium (#S0192; Sigma-Aldrich, St. Louis, MO) supplemented with Insulin-Transferrin-Selenium-X Supplement (ITS) (#51500-056; Invitrogen, Carlsbad, CA). This day was defined as day 0 of differentiation. BMP4 (#314-BP-010; R&D Systems, Minneapolis, MN) was added for first 4 days and replaced by $VEGF_{165}$ (#293-VE-050; R&D Systems) and SCF (#255-SC-050; R&D Systems) on day 4. On day 6, the cytokines were again replaced by the haematopoietic cocktail described in the result section. Concentration of each cytokine was as follows: 20 ng/mL BMP4, 40 ng/mL $VEGF_{165}$, 50 ng/mL SCF, 10 ng/mL TPO (#288-TPN-025; R&D Systems), 50 ng/mL IL3 (#203-IL-050; R&D Systems), 50 ng/mL Flt-3 ligand (#308-FK-025; R&D Systems), 50 ng/mL G-CSF (#214-CS-025; R&D Systems), 50 ng/mL complex of IL-6 and soluble IL-6 receptor (FP6) (kindly provided by Kyowa Hakko Kirin Co., Ltd., Tokyo, Japan) and 5 IU/mL EPO (#329871; EMD Biosciences, San Diego, CA). Thereafter, the medium was changed every 5 days.

Antibodies

The primary murine anti-human monoclonal antibodies used for flow cytometric (FCM) analysis are as follows: PE-conjugated anti-SSEA-4 (#330405; BioLegend, San Diego, CA), Alexa Fluor® 647-conjugated anti-TRA-1-60 (#560122; Becton-Dickinson), biotin-conjugated anti-CD140a (#323503; Biolegend), Alexa Fluor® 647-conjugated anti-KDR (#338909; BioLegend), PE-conjugated anti-CXCR4 (#555974; Becton-Dickinson), PE-conjugated anti-CD117 (#313203; BioLegend), PE-conjugated CD34 (#A07776; Beckman Coulter, Brea, CA), FITC-conjugated CD43 (#560978; Becton-Dickinson), and APC-conjugated CD45 (#IM2473; Beckman Coulter). A streptavidin-PE (#554061; Becton Dickinson) was used as secondary antibody against biotin-conjugated primary antibody. The primary antibodies used to immunostain the colonies and floating blood cells included anti-human Oct3/4 (#611203; Becton-Dickinson), T (#sc-101164; Santa Cruz Biotechnology, Santa Cruz, CA), KDR (#MAB3571; R&D Systems), VE-Cadherin (#AF938; R&D Systems), and rabbit anti-pan-human Hb (#0855129; MP Biomedicals, Solon, OH). FITC-conjugated donkey anti-rat antibodies and Cy3-conjugated goat anti-mouse antibodies (Jackson ImmunoResearch Laboratories, Inc., West Grove, PA) were used as secondary antibodies.

Cytostaining

Floating cells were centrifuged onto glass slides by using a Shandon Cytospin 4 Cytocentrifuge (Thermo, Pittsburgh, PA) and analysed by microscopy after staining with May–Giemsa or myeloperoxidase. For immunofluorescence staining, cells fixed with 4% paraformaldehyde were first permeabilized with phosphate-buffered saline containing 5% skimmed milk (Becton–Dickinson) and 0.1% Triton X-100 and then incubated with primary antibodies, followed by incubation with FITC or Cy3-conjugated secondary antibodies. Nuclei were counterstained with 4,6-diamidino-2-phenylindole (DAPI) (Sigma-Aldrich).

Flow cytometric analysis

The adherent cells were treated with Dispase (#354235; Becton-Dickinson) and harvested by gently scraping the culture dish. Aggregated cell structure was chopped by a pair of scissors, processed by GentleMACS (Milteny Biotec, Germany) and then dispersed by 40-μm strainers (#2340; Becton-Dickinson) before staining with antibodies. Dead cells were excluded by DAPI staining. Samples were analysed using a MACSQuant (Milteny Biotec) and FlowJo software (Thermo). Cell sorting was performed using a FACSVantage or FACSAria (Becton–Dickinson).

RNA extraction and real-time quantitative PCR analysis

RNA samples were prepared using silica gel membrane-based spin-columns (RNeasy Mini-KitTM; Qiagen, Valencia, CA) and subjected to reverse transcription (RT) with a Sensiscript-RT Kit (Qiagen). All procedures were performed according to the manufacturer's instructions. For real-time quantitative PCR, primers and the fluorogenic probes were designed and selected according to Roche Universal Primer library software (Roche Diagnostics) and MGB probe system (Applied Biosystems, Carlsbad, CA). The instrument used was the Applied Biosystems ABIPrism 7900HT sequence detection system, and the software for data collection and analysis was SDS2.3. A GAPDH RNA probe (Hs00266705_g1) was used to normalise the data.

Clonogenic colony-forming assay

At the indicated days of culture, from days 6 through 25, the adherent cells were treated with dispase and harvested. They were incubated in a new tissue-culture dish (#3003, Becton–Dickinson) for 10 min to eliminate adherent non-haematopoietic cells [40]. Floating cells were collected and dispersed by 40-μm strainers. After dead cells were eliminated by labeling with Dead-Cert Nanoparticles (#DC-001, ImmunoSolv, Edinburgh, UK), live hematopoietic cells were cultured at a concentration of 1×10^3 (for counting CFU-G) or 10^4 (for counting CFU-Mix, BFU-E, and CFU-GM) cells/ml in 35-mm petri dishes (#1008; Becton-Dickinson) using

1 ml/dish of MethoCult GF+ semisolid medium (#4435; STEMCELL Technologies) as previously described. Colonies were counted after 14–21 days of incubation, and colony types were determined according to the criteria described previously [41,42,43] by in situ observation using an inverted microscope. The abbreviations used for the clonogenic progenitor cells are as follows: CFU-Mix, mixed colony-forming units; BFU-E, erythroid burst-forming units; CFU-GM, granulocyte–macrophage colony-forming units; and CFU-G, granulocyte colony-forming units.

Single-cell deposition assay

The single-cell deposition assay was performed as described previously [17,18,28]. In brief, single sorted cells were deposited in individual wells of 96-well plates with confluent OP9 layers and cultured for 14 days. Wells were scored by morphological observation for hematopoietic colony detection and stained with anti-vascular endothelial cadherin (VE-cadherin) antibodies for endothelial lineage detection.

Chemotaxis assay

Chemotaxis assay was performed with modified Boyden chamber method using 3.0-μm pore size cell culture inserts (Becton Dickinson). In brief, 5×10^4 cells harvested from floating cell fraction at day 25 were added to the upper chamber and induced to migrate towards the lower chamber containing 10 nM formyl-Met-Leu-Phe (fMLP; Sigma-Aldrich) for 4 hours at 37°C. After incubation, the cells in the lower chamber were collected and counted using a MACSQuant flow cytometer (Miltenyi Biotec). For quantitative analysis, equivalent amount of 6-μm beads (Becton Dickinson) were added to each FCM sample, and the cell numbers were determined by measuring the ratio of cells to beads.

Phagocytosis and detection of reactive oxygen species

Phagocytosis and production of reactive oxygen species were detected by chemiluminescent microspheres (luminol-binding carboxyl hydrophilic microspheres; TORAY, Tokyo, Japan) as described previously [44]. In brief, 2×10^4 floating cells were suspended in 50 μL of the reaction buffer (HBSS containing 20 mM *N*-2-hydroxyethylpiperazine-*N*-2-ethanesulfonic acid (HEPES)) per tube. To activate the system, 5 μl chemiluminescent microspheres were added, and light emission was recorded continuously using a luminometer (TD-20/20; Turner Designs, Sunnyvale, CA). During the measurement, samples were kept at 37°C. To inhibit the reaction, 1.75 μg of cytochalasin B (Sigma-Aldrich) was added to the samples.

Measurement of oxygen-binding ability

Floating blood cells derived from KhES-1 and 253G4 strains were harvested on day 32 of differentiation (with erythropoietic cytokine cocktail). Oxygen dissociation curves for hemoglobin were measured using a Hemox-Analyzer (TCS Scientific Corporation, New Hope, PA) as previously reported [45,46].

Results

Stepwise generation of functional hematopoietic cells from human ES/iPS cells in the serum-free monolayer culture without animal-derived stromal cells

To assess the differentiation activity of each human ES/iPS cell line with high reproducibility, we used a chemically defined medium in the monolayer differentiation culture and succeeded in inducing various blood cells, including erythrocytes and neutrophils (Figure 1a). To present the developmental process from human ES/iPS cells to blood cells in an orderly manner, we divided the entire process into 3 steps: (1) initial differentiation into PS cells, (2) induction of the hematopoietic mesoderm (Movie S1), and (3) commitment to the hematopoietic lineages (Movie S2).

Step 1: Induction of PS-like cells from undifferentiated human ES/iPS cells with BMP4 (days 0–4). First, we examined the efficacy of initial progression from undifferentiated pluripotent cells (KhES-1) into PS-like cells according to the expression of representative marker genes, such as *T* and *Mixl1* (Figure 1b), and the change in morphology (Figure 1c). Without cytokines, these genes were only slightly upregulated during the first 4 days. However, when 40 ng/mL BMP4 was added to the culture, the expression levels of these genes increased, which is compatible with previous reports on the importance of BMP4 in mesodermal/endodermal differentiation via PS during early embryogenesis (Figure 1b). Further, transcription levels of the undifferentiated marker *Nanog* decreased. During this period, the colonies showed substantial morphological changes at the margins, and cell density decreased and cell contact diminished (Movie S1, Figure 1c). Immunohistochemical staining assays confirmed the upregulation of T and the lateral mesodermal marker, KDR, and downregulation of Oct3/4 (Figure 1c). However, regarding ectodermal commitment, the representative marker gene *Sox1* was hardly detected on day 4 in the presence of BMP4 (Figure 1b).

To assess the role of BMP4 in this step, we analyzed the differentiation efficacy of individual ES (KhES-1 and KhES-3) and iPS (201B7 and 253G4) cell strains with various concentrations of BMP4 in the presence or absence of its inhibitor, Noggin. As shown in Figure 1d, *T* gene expression was upregulated by BMP4 dose-dependently up to 20 ng/mL and was almost completely suppressed by the BMP4 inhibitor, Noggin, in both ES and iPS cells. This suggested that BMP4 was critical at this stage. From these results, we used BMP4 at 20 ng/mL concentration in subsequent experiments.

We also assayed the expression of several cell surface protein markers in this step (Figure 1e). On day 4, undifferentiated cell markers (TRA-1-60 and SSEA4) were downregulated, whereas paraxial and lateral mesoderm cell markers (CD140a and KDR) and markers for mesodermal and hematopoietic progenitors (CXCR4 and CD117) were upregulated. The early-phase hematopoietic-committed cell markers (CD34 and CD43) were still negative at this stage. Similar results were obtained for both ES and iPS cells (data not shown), suggesting that our system initiated paraxial and lateral mesodermal differentiation from pluripotent stem cells during Step 1 [33].

Step 2: Generation of $KDR^+CD34^+CD45^-$ progenitors with VEGF and SCF (days 4–6). Our previous studies of primate ES cells demonstrated that $KDR^+CD34^+CD45^-$ mesodermal progenitors derived in a VEGF-containing culture on OP9 stromal cells included hematopoietic progenitors [17,18]. Therefore, we used this data to induce these progenitors in our culture system. Considering the partial expression of KDR and CD117 during the first step, we replaced BMP4 with 40 ng/mL $VEGF_{165}$ (ligand for KDR) and 50 ng/mL SCF (ligand for CD117) on day 4 to accelerate selective differentiation to the lateral mesoderm with hematopoietic activities (Figure 1a).

During the next 2 days, the colonies exhibited 2 distinct regions: a plateau-like central area with stratified components and a surrounding area with monolayer cells (Movie S1, Figure 1c). On day 6, the mRNA expression pattern indicated the dominance of mesodermal cells rather than endodermal or ectodermal lineages

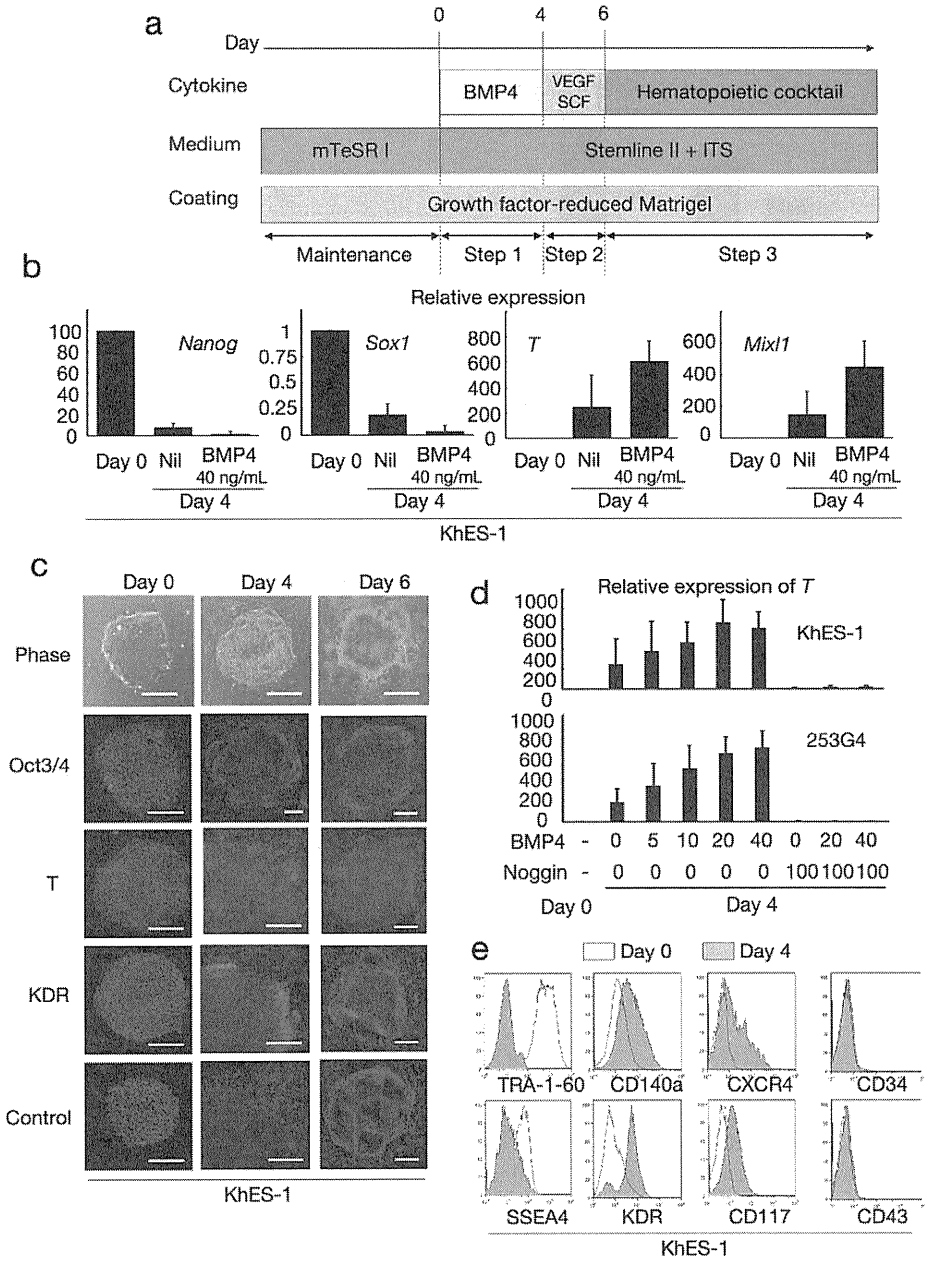

Figure 1. Blood cell induction from pluripotent stem cells starts with commitment into primitive streak. a. A schema of stepwise haematopoietic differentiation of human ES/iPS cells. **b.** Gene expression analysis of colonies at the beginning of differentiation (day 0) and the end of step 1 (day 4) with/without 40 ng/mL BMP4. Data from KhES-1 are shown as representative. **c.** Phase contrast microscopies and immunofluorescence staining of colonies during initial differentiation. Data from KhES-1 are shown as representative. **d.** Relative expression of *T* at day 4 of differentiation with different combinations of BMP4 and its inhibitor Noggin. Where shown, bars represent standard deviation of the mean of three independent experiments; Scale bars, 500 μm. Data from KhES-1 and 253G4 strains are shown as representative. **e.** Flow cytometric analysis of differentiating cells on day 4, indicating the down-regulation of immature cell markers and up-regulation of differentiated progenitor markers. Data from KhES-1 are shown as representative.
doi:10.1371/journal.pone.0022261.g001

(Figure 2a), and flow cytometric (FCM) analysis demonstrated the emergence of new cell fractions that were positive for KDR, CD117, CXCR4, and CD34 but negative for CD140a, CD43, and CD45 (Figure 2b). Our system robustly supports mesodermal induction from both ES and iPS cells, despite differences in efficacy among cell strains (Figure 2c).

Further, immunohistochemical staining for KDR indicated an uneven distribution of KDR^+ cells at the marginal zone of the plateau area (Figure 1c), suggesting that differentiation polarity within the colonies resulted in site-specific emergence of putative hematopoietic mesodermal progenitors.

Step 3: Production of functional blood cells dependent on cytokine cocktails (day 6 onward). On day 6, we changed the culture medium to another chemically defined medium containing hematopoietic cytokines (Figure 1a). To achieve lineage-directed differentiation, we used 2 combinations of cytokines: a myeloid-

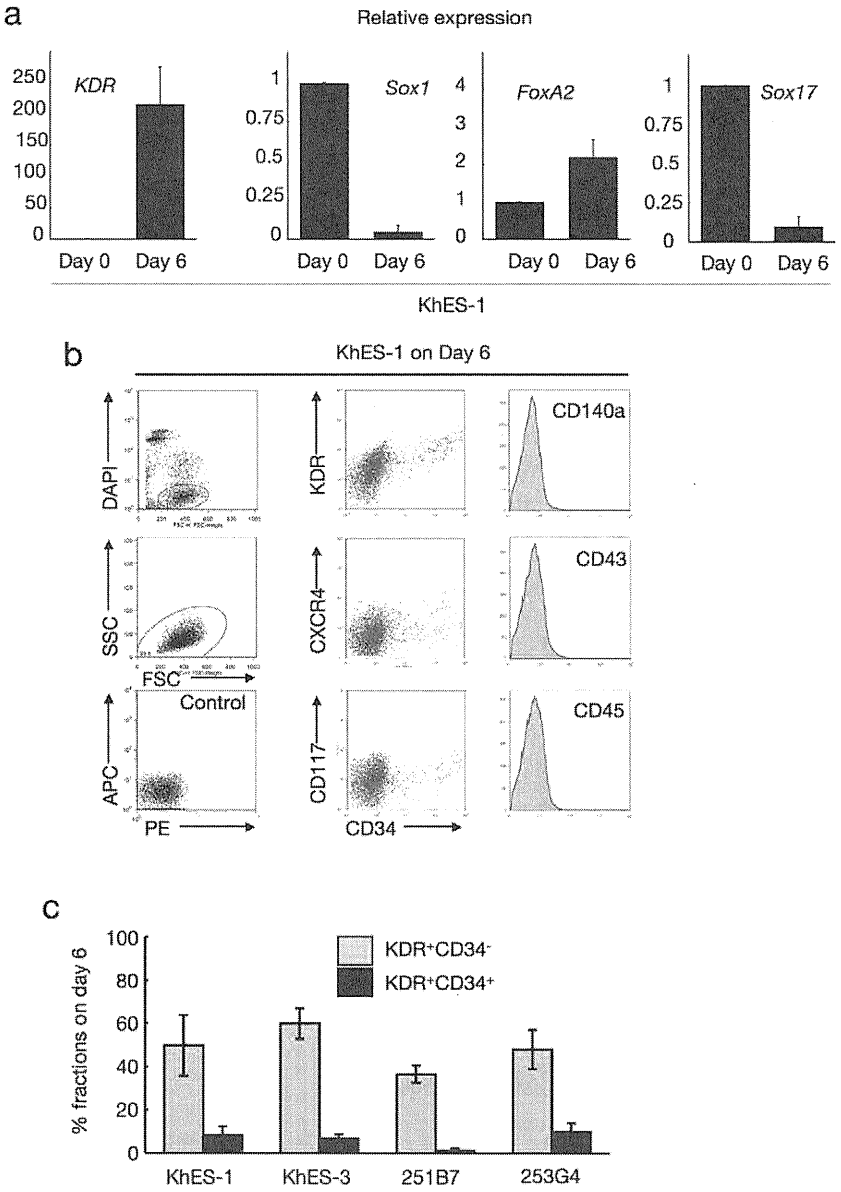

Figure 2. Characterization of cells during initial differentiation with lineage-specific marker expression. a. Expression analysis of lineage-specific marker genes at the beginning of differentiation (day 0) and the end of step 2 (day 6). Bars represent standard deviation of the mean of three independent experiments. Data from KhES-1 are shown as representative. **b.** The development of progenitors on day 6 positive for lateral mesoderm markers but negative for paraxial mesoderm and haematopoietic cell markers. Leftmost column shows the gating strategy for eliminating dead cells and debris. Data from KhES-1 are shown as representative. c. Efficacy of inducing $KDR^{+}CD34^{+\text{ or }-}$ mesodermal progenitors from each two lines of human ES cells and iPS cells. Bars represent standard deviation of the mean of three independent experiments.
doi:10.1371/journal.pone.0022261.g002

induction cocktail containing SCF, TPO, IL3, FLT-3 ligand, and G-CSF; and an erythropoietic-differentiation cocktail containing SCF, TPO, IL3, FP6, and EPO.

Regardless of the cocktails, the colonies first exhibited a rosary-like appearance, with small sac-like structures aligned along the margins of the plateau areas, and grew for several days (Figure 3a, left panel). Hematopoietic cell clusters emerged from the edge of these structures on days 10–12, followed by the appearance of floating blood cells a few days later, which increased thereafter; hematopoietic clusters grew in size and number, and some exhibited areas with a cobblestone-like appearance (Figure 3a, right 3 panels; Movie S2). When fresh medium with the cytokines was supplied every 5 days, blood cell production was observed in both ES and iPS cell experiments until day 50 of differentiation, whereas few hematopoietic cells appeared without the cytokines (data not shown).

As expected, the myeloid-induction cocktail induced myelomonocytic lineages predominantly positive for CD45. Blood cells harvested on day 30 exhibited morphology compatible with myelomonocytic precursors and mature neutrophils, and displayed positive myeloperoxidase staining (Figure 3b). On the other hand, the erythropoietic-differentiation cocktail yielded cell lineages that included hemoglobin-positive (Hb^{+}) erythroid cells and $CD41^{+}$ megakaryocytes (Figure 3b). In the KhES-1 strain (3.5 [standard deviation (SD) = 1.5] undifferentiated colonies 250 μmm in diameter were initially plated in individual wells of 6-well plates

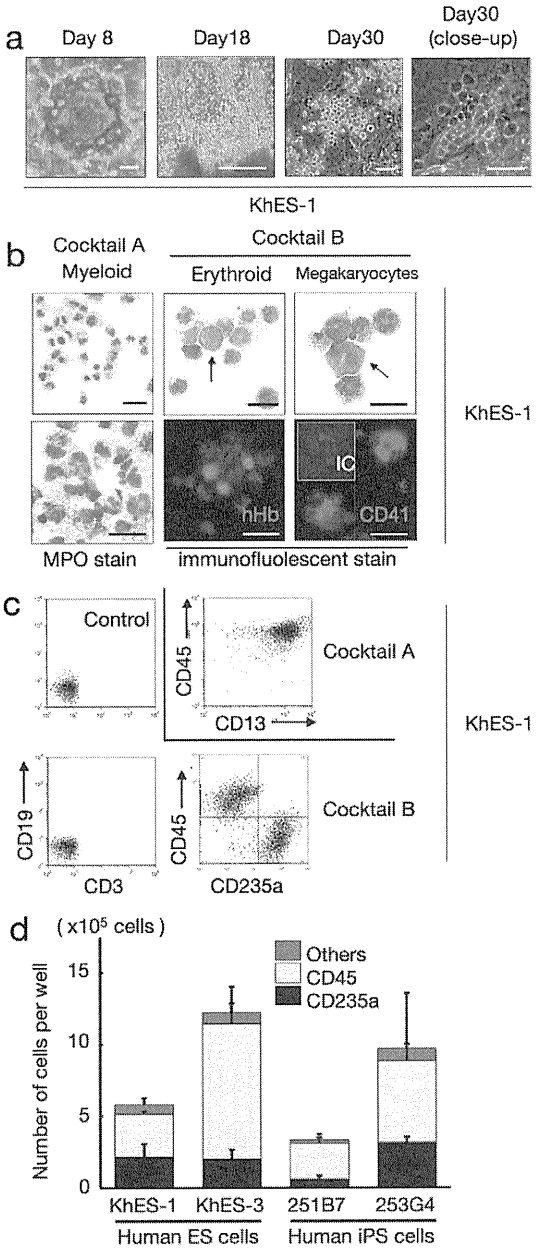

Figure 3. Human ES/iPS cell-derived haematopoiesis in a monolayer culture free from animal serum or stromal cells. a. Sequential phase contrast pictures showing haematopoietic development. Scale bars, 500 μm (left two panels) and 100 μm (right two panels). Data from KhES-1 are shown as representative. **b.** Floating cells harvested on day 30 showing various lineages of haematopoietic cells; MPO-positive myeloid lineage cells (leftmost panels), pan-human Hb-positive erythroid lineage cells (centre panels), and CD41-positive megakaryocytes (rightmost panels). Scale bars, 100 μm. Data from KhES-1 are shown as representative. **c.** Expression of lineage-specific antigens on floating cells harvested on day 30; Myeloid lineages (CD13 and CD45), erythroid lineages (CD235a), T cells (CD3), and B cells (CD19). Data from KhES-1 are shown as representative. **d.** Numbers and fraction of blood cells induced from each two lines of human ES cells and iPS cells. Bars represent standard deviation of the mean of three independent experiments.
doi:10.1371/journal.pone.0022261.g003

at the start of differentiation), counting and FCM analysis of harvested blood cells on day 30 revealed the existence of 7.7×10^5 (SD = 2.3×10^5) different cell lineages per well, including 36.0% (SD = 6.4%) $CD235a^+$ erythroid and 53.2% (SD = 9.4%) $CD45^+$ myelomonocytic lineages, but no lymphoid lineage cells (Figure 3c). Although the differentiation efficacy and lineage distribution depend not only on the cytokines but also on the cell strains, the data indicates that human ES and iPS cells develop into various lineages of hematopoietic cells, robustly and orderly, in our novel monolayer culture system without xeno-derived serum or stromal cells (Figure 3d).

ES/iPS cell-derived hematopoietic cells have similar potential to in vivo-derived blood cells in function

Considering the use of ES/iPS cell-derived hematopoiesis for various clinical and research applications, it is important to confirm the function of the generated blood cells. Neutrophils derived with the myeloid-induction cocktail exhibited migration activity in response to the chemoattractant fMLP (Figure 4a) and phagosome-dependent reactive oxygen production, which was inhibited by the phagosome destruction agent, cytochalasin B (Figure 4b). On the other hand, erythroid lineage cells derived with the erythropoietic-differentiation cocktail (harvested on day 32 of differentiation) exhibited an oxygen dissociation curve that was similar, despite being slightly left-shifted, to those obtained with adult and cord blood cells (Figure 4c). These data indicate that our culture facilitates robust and orderly development of human ES and iPS cells into functional hematopoietic cells with similar potential to in vivo-derived blood cells.

Clonogenic hematopoietic development from human ES/iPS cell-derived progenitors

The human hematopoietic system is a hierarchy of various component cells from stem or progenitor cells to terminally differentiated cells. For example, $CD34^+$ cells in umbilical cord blood or bone marrow contain putative hematopoietic stem cells and are used as a source of stem cell transplantation. The identification and proliferation of such cells in vitro have been of great interest in medical science research.

To assess the potential of our system for supporting generated immature stem or progenitor cells, we evaluated the colony-forming ability of the cultivated hematopoietic progenitors in the system. Accordingly, the cells were cultured with SCF, TPO, IL3, FLT-3 ligand, and FP6. In these conditions, $CD34^+CD45^+$ hematopoietic cells existed up to day 25, indicating that the immature hematopoietic cells can be maintained in our serum-free culture (Figure 5a).

We harvested adherent blood cells from the previously described culture and transferred them into a methylcellulose-containing medium to perform colony-forming assays with SCF, TPO, IL3, G-CSF, and EPO. As shown in Figure 5b and c, CFU-Mix, BFU-E, CFU-GM, and CFU-G colonies developed from plated cells. The total number of colonies increased dramatically from day 6 to day 10, then gradually increased until day 15 and decreased thereafter. CFU-Mix and BFU-E colonies were mainly observed until day 15 and were thereafter replaced by CFU-GM and CFU-G colonies. Similar tendencies were observed in both ES and iPS cells. These results suggest that our culture system can incubate multipotent hematopoietic stem or progenitor cells over a period of time.

Identification of $KDR^+CD34^+CD45^-$ bipotential hemoangiogenic progenitors derived in serum-free conditions

During embryogenesis, hematopoietic development is closely associated with endothelial lineage commitment [47,48], and

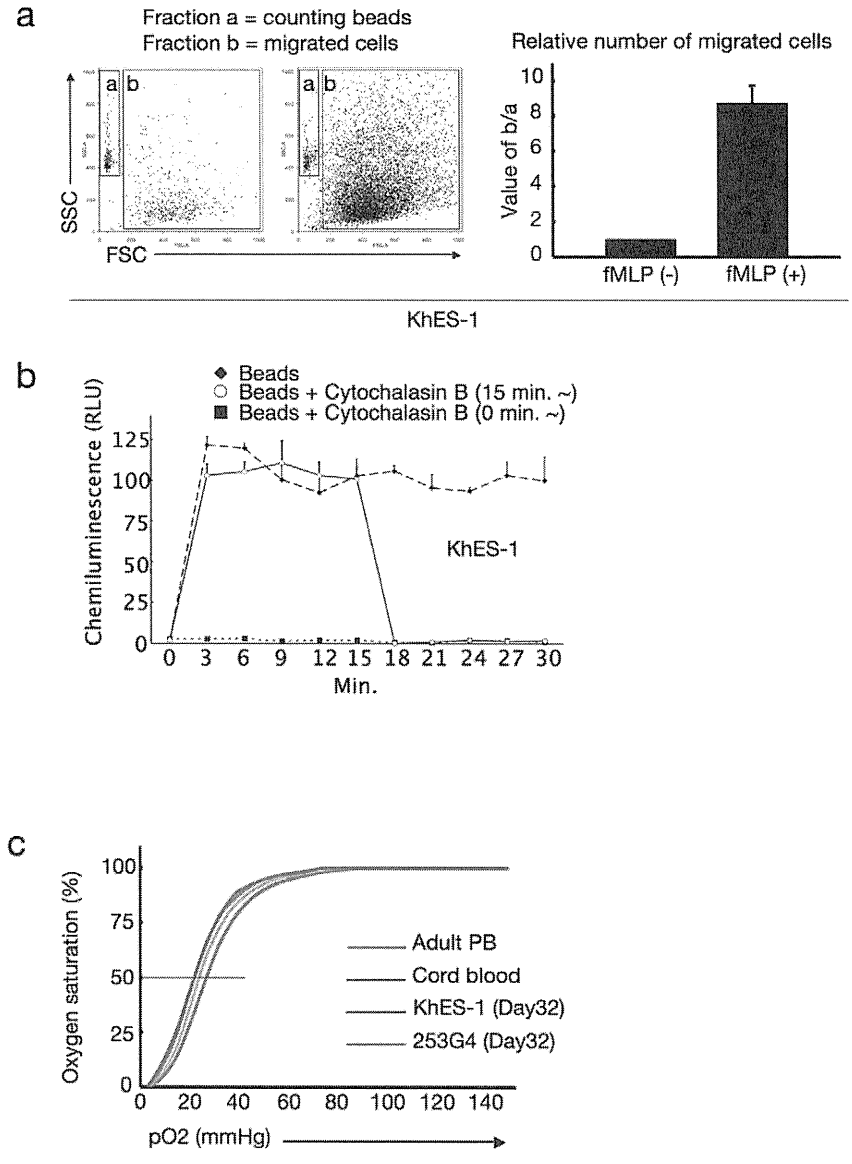

Figure 4. Functional blood cells derived from human ES/iPS cells. a. Number of migrated cells that permeated through the transwell membrane with or without fMLP. Values were normalised to the number of counting beads, and the control values were arbitrarily set to the condition without fMLP. Data from KhES-1 are shown as representative. **b.** Assay for phagocytosis-induced respiratory burst activity using chemiluminescent microspheres (luminol-binding microspheres). Abbreviation: RLU, relative light units. Data from KhES-1 are shown as representative. **c.** Oxygen dissociation curves of erythroid cells derived from human ES/iPS cells (harvested on day32 of differentiation), human cord blood, and adult peripheral blood. Where shown, bars represent standard deviation of the mean of three independent experiments.
doi:10.1371/journal.pone.0022261.g004

previous studies have demonstrated that ES cells can differentiate into the common multipotent progenitors that differentiate into both blood and endothelial cells at the single cell level on OP9 stroma [17,28,49]. Although the experiments described thus far demonstrated that the serum-free, xeno-cell-free culture condition supported human ES/iPS cell-derived hematopoiesis in an orderly manner, as observed during embryogenesis, it was unclear which day 6 fraction(s) developed into blood cells. To clarify this point, human ES cells stably expressing green fluorescent protein (GFP) were cultured, then 1×10^4 cells of $GFP^+KDR^-CD34^-CD45^-$ (Fraction A), $GFP^+KDR^+CD34^-CD45^-$ (Fraction B), and $GFP^+KDR^+CD34^+CD45^-$ (Fraction C) fractions were transferred on day 6 into a synchronous differentiation culture of unlabeled ES cells (Figure 6a). Nineteen days later (day 25 of differentiation), GFP^+ small round cell-containing colonies were observed predominantly in Fractions B and C, and FCM analysis of the entire culture confirmed the emergence of GFP^+CD45^+ cells mainly from Fraction C (Figure 6b). On the other hand, few blood cells positive for GFP were generated from Fraction A. These results were obtained with 2 independent strains of human ES cells (KhES1-EGFPneo on KhES-1 and KhES3-EGFPneo on KhES-3) (Figure 6c) and indicated that hematopoietic progenitors were present in the KDR^+ fraction, particularly in the KDR^+CD34^+ fraction, on day 6 of differentiation.

Finally, we performed a single-cell deposition assay by transferring single sorted human ES/iPS cell-derived $GFP^+KDR^+CD34^+CD45^-$ cells, which were negative for VE-cadherin, on day 6 into individual wells of 96-well plates coated

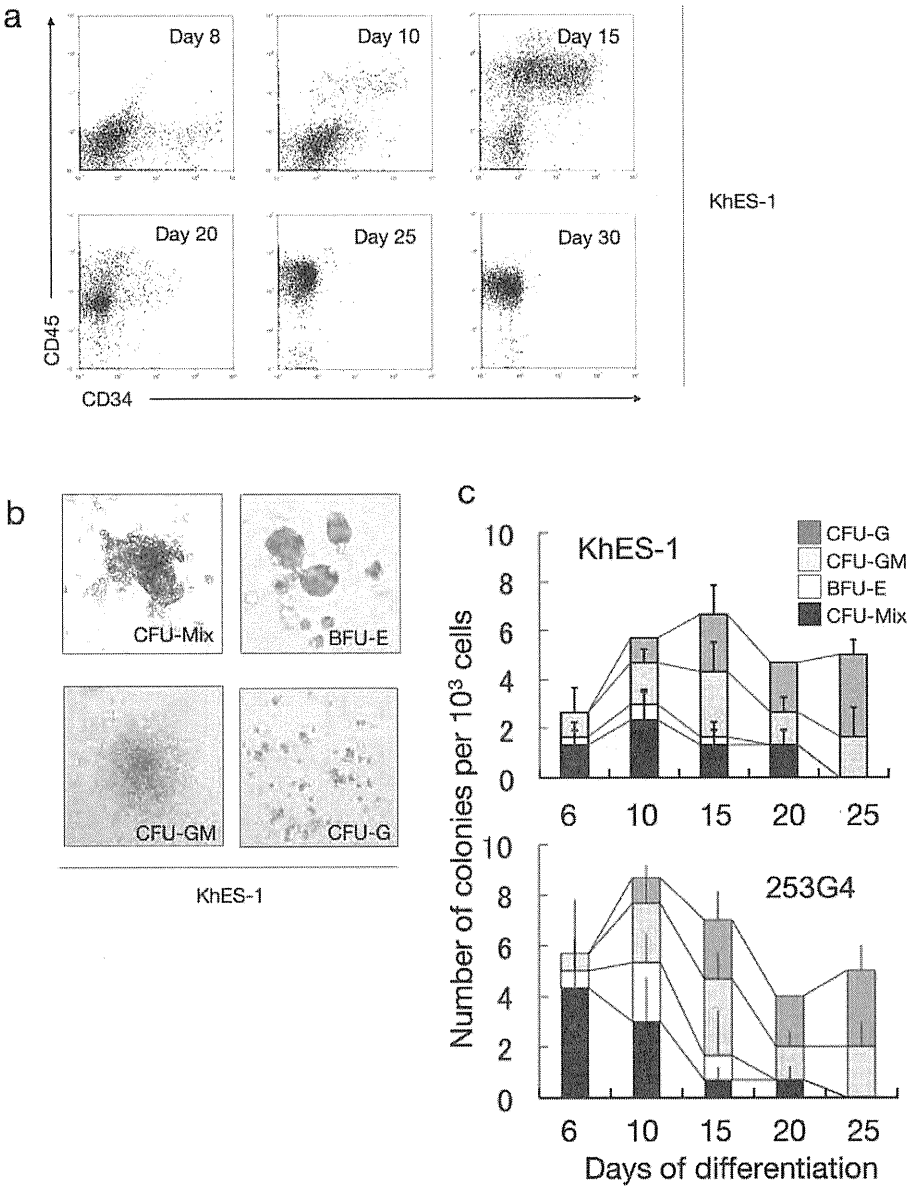

Figure 5. Hematopoietic stem/progenitor cells in culture. a. Sequential FCM analysis of cells harvested on indicated days showing the existence of $CD34^{+}CD45^{+}$ haematopoietic progenitor cells in culture. Data from KhES-1 are shown as representative. **b.** Various colony types on MTC-containing medium clonally emerged from single haematopoietic progenitor cells. Data from KhES-1 are shown as representative. **c.** Numbers of each colony type derived from different days of culture. Bars represent standard deviation of the mean of three independent experiments. Data from KhES-1 and 253G4 strains are shown as representative.
doi:10.1371/journal.pone.0022261.g005

with an OP9 cell layer. As shown in Figure 6d and e, the proportion of hematopoietic cell (HC) development, VE-cadherin^{+} endothelial cell (EC) development, and HC plus EC development on day 20 were 9.0%, 6.8%, and 4.0%, respectively, for KhES-1 and 11.6%, 12.7%, and 8.3%, respectively, for 253G4 iPS cells. These results demonstrate that the common mesodermal progenitors that can differentiate into both blood and endothelial cells at the single-cell level are induced in our culture condition.

Discussion

In this study, we demonstrated the orderly mesodermal and hematopoietic differentiation of human ES and iPS cells in a novel serum-free monolayer culture condition. Simple manipulation of cytokine combinations facilitated robust, reproducible, and highly directed stepwise commitment to specific lineages of functional blood cells.

There are several reports on hematopoietic differentiation of human ES/iPS cells, such as murine-derived OP9 stromal cell coculture and feeder/serum-free EB formation systems [20,22,23,24,30,31,32,50]. However, two-dimensional cultures containing xeno-serum/cells often cause dependency on their lots, while complicated three-dimensional structures inside EBs make it difficult to assess and control conditions for inducing specific progenitors. Actually, few in vitro systems have been able to reliably reproduce hematopoietic development from mesodermal progenitors or model the in vivo coexistence of developing hematopoietic cells and their autologous microenvironments in

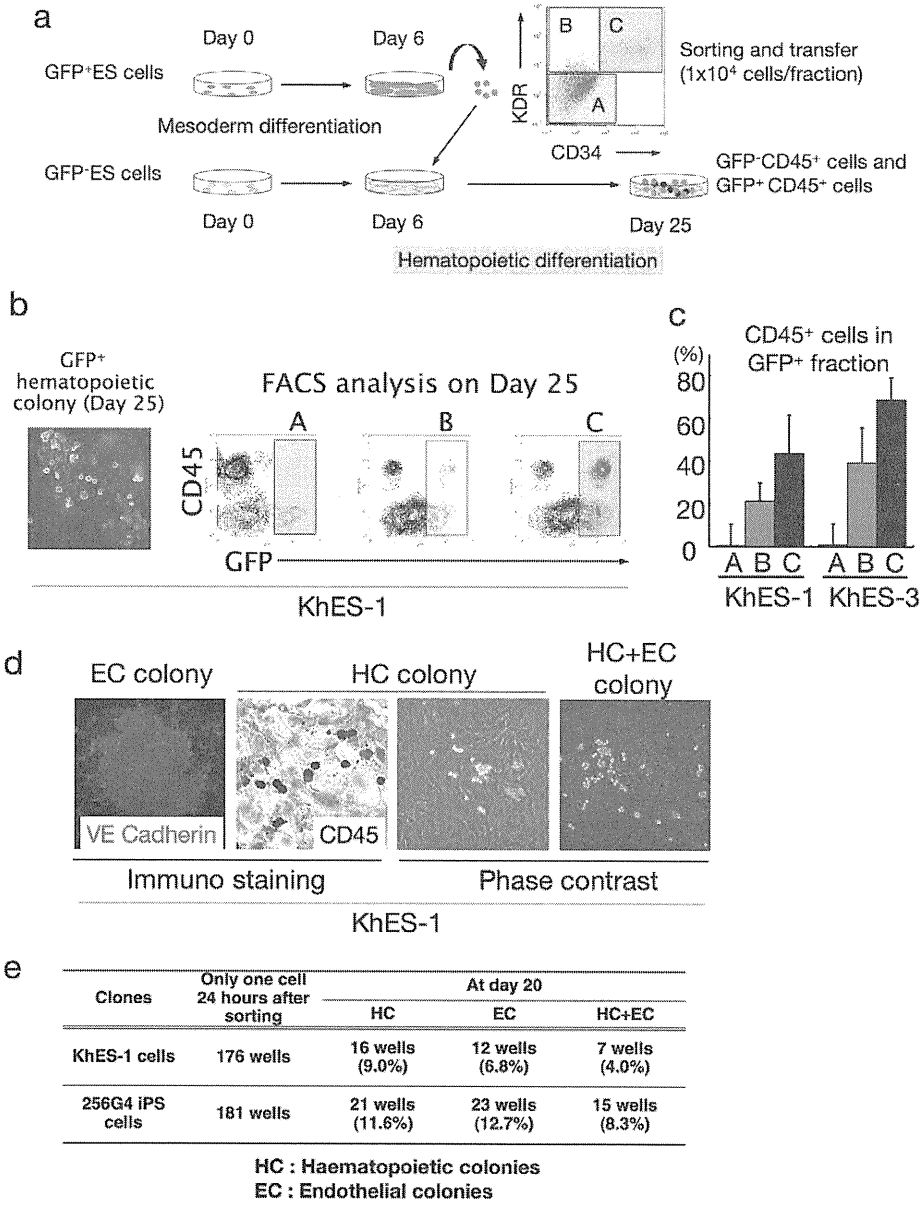

e

Clones	Only one cell 24 hours after sorting	At day 20		
		HC	EC	HC+EC
KhES-1 cells	176 wells	16 wells (9.0%)	12 wells (6.8%)	7 wells (4.0%)
256G4 iPS cells	181 wells	21 wells (11.6%)	23 wells (12.7%)	15 wells (8.3%)

HC : Haematopoietic colonies
EC : Endothelial colonies

Figure 6. Haematopoietic differentiation from KDR$^+$CD34$^+$ mesodermal progenitors. a. Schema of the protocol for measuring haematopoietic activities of depicted fractions on day 6. **b.** Each sorted fraction-derived haematopoiesis on day 25 detected by fluorescent microscopy and FCM analysis. Data from KhES-1 are shown as representative. **c.** Ratio of CD45$^+$ cells in GFP$^+$ fraction on day 25 showing the strongest haematopoietic activity of fraction C followed by fraction B. **d.** Single KDR$^+$CD34$^+$CD45$^-$ cell-derived haematopoietic colonies (HC), VE-cadherin$^+$ endothelial colonies (EC), and HC+EC colonies generated on OP9 cell layers. Data from KhES-1 are shown as representative. **e.** Number of wells that showed HC, EC, and EC+HC development.
doi:10.1371/journal.pone.0022261.g006

serum-free conditions. Our less labor-intensive and clearly defined monolayer culture facilitates observation of the stepwise development of pluripotent cells to blood cells via common hemoangiogenic progenitors and the behavior of hematopoietic cells on autologous stromal cells. Consequently, assays for elucidating differences in lineage specification of various ES/iPS cell strains, including hematopoietic potential, can be performed with high reproducibility. This is particularly important because individual pluripotent cell strains vary in differentiation potentials [51,52,53]. This study demonstrated quantitative differences in hematopoietic differentiation efficacy and lineage commitment among 4 ES/iPS cell strains.

Because human ES/iPS cells are feasible cell sources for various clinical applications, scientific and medical communities have shown continuing interest in hematopoietic stem cell induction from ES/iPS cells. Previous trials have indicated that murine ES cell-derived hematopoietic cells overexpressing HoxB4 [54] can replenish the bone marrow of lethally irradiated recipient mice. However, it remains a challenge to develop bona fide human hematopoietic stem cells with bone marrow reconstitution activity at the single-cell level. In our study, we observed many cobblestone area-forming cells, which reportedly indicate the existence of very immature hematopoietic progenitors. Moreover, FCM analyses and colony-forming assays suggested that ES and iPS human cell-

derived hematopoiesis in our method occurs through clonogenic hematopoietic stem/progenitor cells. We are in the process of determining in vivo repopulating ability of cells harvested from our culture by using serial transplantation into immunodeficient mice to assess the possibility of inducing feasible cell sources for various clinical applications, such as cell therapies and disease investigation.

Finally, time-lapse imaging strongly indicated crosstalk between hematopoietic cells and the autologous microenvironment composed of non-hematopoietic cells. Emerged blood cells move about actively and generate colonies in surrounding cell layers, suggesting the importance of a direct interaction between blood cells and microenvironmental cells for the maintenance, proliferation, and differentiation of stem or progenitor cells (Movie S3). In fact, a model of hematopoietic disorders triggered by mutation in the bone marrow microenvironment has been recently reported [55]. However, further investigation is necessary to identify the mechanisms responsible for such phenomena. Our culture may aid these investigations as it facilitates simple and sequential harvest of hematopoietic cells with minimal contamination by autologous adherent cell layers.

In conclusion, this study presents novel methods for analyzing the mechanisms of normal hematopoiesis in a robust, reproducible, and stepwise manner. Furthermore, employing gene-manipulated ES cells or disease-specific iPS cells will supply in vitro models of disease pathology, thereby providing further insights into hematological defects in conditions such as aplastic anemia and myelodysplastic syndromes.

Supporting Information

Movie S1 Time-lapse microscopic movie showing the morphological change in a single colony from day 0 to day 6 (initial differentiation). In this period, a colony begins forming a rosary-like morphology as it differentiates. The pictures were automatically taken every 8 minute by Biostation IM (Nikon Instruments, Tokyo, Japan).
(MOV)

Movie S2 Time-lapse microscopic movie showing the morphological change in a single colony from day 6 to day 25 (hematopoietic differentiation). After adding hematopoietic cytokines on day 6, hematopoietic cells first emerge from the areas near the edge of stratified zone. The pictures were automatically taken every 8 minute by Biostation IM (Nikon Instruments, Tokyo, Japan).
(MOV)

Movie S3 Close-up time-lapse microscopic movie showing hematopoietic cells moving about and generating colonies in surrounding cell layers. The pictures were automatically taken every 8 minute by Biostation IM (Nikon Instruments, Tokyo, Japan).
(MOV)

Acknowledgments

We are grateful to Kyowa Hakko Kirin Co. Ltd. for providing FP6. We thank N. Nakatsuji (Institute for Frontier Medical Sciences, Kyoto University) for providing human ES cells and S. Yamanaka (CiRA) for providing human iPS cells. We thank T. Tanaka (Nakahata-ken, CiRA) for his advice on undifferentiated human ES/iPS cell culture; T. Morishima (Graduate school of medicine, Kyoto University) for instructing the function assay of neutrophils; Y. Sasaki, S. Tomida, M. Yamane, and Y. Shima (Nakahata-ken, CiRA) for their excellent technical assistance; and H. Koyanagi (Nakahata-ken, CiRA), N. Hirakawa, Y. Ogihara, and G. Odani (Nikon Instruments Company) for their expertise in microscopic time-lapse monitoring. We thank H. Watanabe (Nakahata-ken, CiRA), M. Muraki, M. Terada, H. Konishi, C. Kaji, N. Takasu, and Y. Takao (Kenkyu-Senryaku-honbu, CiRA) for their superb administrative assistance.

Author Contributions

Conceived and designed the experiments: AN TH KU TN MKS. Performed the experiments: AN H. Sakai. Analyzed the data: AN TH KU KO IK H. Sakai. TN MKS. Contributed reagents/materials/analysis tools: H. Suemori H. Sakai. Wrote the manuscript: AN TN MKS.

References

1. Evans MJ, Kaufman MH (1981) Establishment in culture of pluripotential cells from mouse embryos. Nature 292: 154–156.
2. Thomson JA, Itskovitz-Eldor J, Shapiro SS, Waknitz MA, Swiergiel JJ, et al. (1998) Embryonic stem cell lines derived from human blastocysts. Science 282: 1145–1147.
3. Keller G (2005) Embryonic stem cell differentiation: emergence of a new era in biology and medicine. Genes Dev 19: 1129–1155.
4. Xu Y, Shi Y, Ding S (2008) A chemical approach to stem-cell biology and regenerative medicine. Nature 453: 338–344.
5. Shi Y, Do JT, Desponts C, Hahm HS, Scholer HR, et al. (2008) A combined chemical and genetic approach for the generation of induced pluripotent stem cells. Cell Stem Cell 2: 525–528.
6. Jaenisch R, Young R (2008) Stem cells, the molecular circuitry of pluripotency and nuclear reprogramming. Cell 132: 567–582.
7. Meissner A, Wernig M, Jaenisch R (2007) Direct reprogramming of genetically unmodified fibroblasts into pluripotent stem cells. Nat Biotechnol 25: 1177–1181.
8. Garcia-Porrero JA, Manaia A, Jimeno J, Lasky LL, Dieterlen-Lievre F, et al. (1998) Antigenic profiles of endothelial and hemopoietic lineages in murine intraembryonic hemogenic sites. Dev Comp Immunol 22: 303–319.
9. Choi K, Kennedy M, Kazarov A, Papadimitriou JC, Keller G (1998) A common precursor for hematopoietic and endothelial cells. Development 125: 725–732.
10. Wood HB, May G, Healy L, Enver T, Morriss-Kay GM (1997) CD34 expression patterns during early mouse development are related to modes of blood vessel formation and reveal additional sites of hematopoiesis. Blood 90: 2300–2311.
11. Shalaby F, Ho J, Stanford WL, Fischer KD, Schuh AC, et al. (1997) A requirement for Flk1 in primitive and definitive hematopoiesis and vasculogenesis. Cell 89: 981–990.
12. Sumi T, Tsuneyoshi N, Nakatsuji N, Suemori H (2008) Defining early lineage specification of human embryonic stem cells by the orchestrated balance of canonical Wnt/beta-catenin, Activin/Nodal and BMP signaling. Development 135: 2969–2979.
13. Flamme I, Breier G, Risau W (1995) Vascular endothelial growth factor (VEGF) and VEGF receptor 2 (flk-1) are expressed during vasculogenesis and vascular differentiation in the quail embryo. Dev Biol 169: 699–712.
14. Risau W (1995) Differentiation of endothelium. FASEB J 9: 926–933.
15. Risau W, Hallmann R, Albrecht U (1986) Differentiation-dependent expression of proteins in brain endothelium during development of the blood-brain barrier. Dev Biol 117: 537–545.
16. Huber TL, Kouskoff V, Fehling HJ, Palis J, Keller G (2004) Haemangioblast commitment is initiated in the primitive streak of the mouse embryo. Nature 432: 625–630.
17. Umeda K, Heike T, Yoshimoto M, Shiota M, Suemori H, et al. (2004) Development of primitive and definitive hematopoiesis from nonhuman primate embryonic stem cells in vitro. Development 131: 1869–1879.
18. Umeda K, Heike T, Yoshimoto M, Shinoda G, Shiota M, et al. (2006) Identification and characterization of hemoangiogenic progenitors during cynomolgus monkey embryonic stem cell differentiation. Stem Cells 24: 1348–1358.
19. Ji P, Jayapal SR, Lodish HF (2008) Enucleation of cultured mouse fetal erythroblasts requires Rac GTPases and mDia2. Nat Cell Biol 10: 314–321.
20. Vodyanik MA, Bork JA, Thomson JA, Slukvin II (2005) Human embryonic stem cell-derived CD34+ cells: efficient production in the coculture with OP9 stromal cells and analysis of lymphohematopoietic potential. Blood 105: 617–626.
21. Kitajima K, Tanaka M, Zheng J, Yen H, Sato A, et al. (2006) Redirecting differentiation of hematopoietic progenitors by a transcription factor, GATA-2. Blood 107: 1857–1863.
22. Takayama N, Nishikii H, Usui J, Tsukui H, Sawaguchi A, et al. (2008) Generation of functional platelets from human embryonic stem cells in vitro via ES-sacs, VEGF-promoted structures that concentrate hematopoietic progenitors. Blood 111: 5298–5306.

23. Choi KD, Vodyanik MA, Slukvin II (2009) Generation of mature human myelomonocytic cells through expansion and differentiation of pluripotent stem cell-derived lin-CD34+CD43+CD45+ progenitors. J Clin Invest 119: 2818–2829.
24. Choi KD, Yu J, Smuga-Otto K, Salvagiotto G, Rehrauer W, et al. (2009) Hematopoietic and endothelial differentiation of human induced pluripotent stem cells. Stem Cells 27: 559–567.
25. Niwa A, Umeda K, Chang H, Saito M, Okita K, et al. (2009) Orderly hematopoietic development of induced pluripotent stem cells via Flk-1(+) hemoangiogenic progenitors. J Cell Physiol 221: 367–377.
26. Timmermans F, Velghe I, Vanwalleghem L, De Smedt M, Van Coppernolle S, et al. (2009) Generation of T cells from human embryonic stem cell-derived hematopoietic zones. J Immunol 182: 6879–6888.
27. Morishima T, Watanabe K, Niwa A, Fujino H, Matsubara H, et al. (2011) Neutrophil differentiation from human-induced pluripotent stem cells. J Cell Physiol 226: 1283–1291.
28. Shinoda G, Umeda K, Heike T, Arai M, Niwa A, et al. (2007) alpha4-Integrin(+) endothelium derived from primate embryonic stem cells generates primitive and definitive hematopoietic cells. Blood 109: 2406–2415.
29. Ji J, Vijayaragavan K, Bosse M, Menendez P, Weisel K, et al. (2008) OP9 stroma augments survival of hematopoietic precursors and progenitors during hematopoietic differentiation from human embryonic stem cells. Stem Cells 26: 2485–2495.
30. Chadwick K, Wang L, Li L, Menendez P, Murdoch B, et al. (2003) Cytokines and BMP-4 promote hematopoietic differentiation of human embryonic stem cells. Blood 102: 906–915.
31. Wang L, Li L, Shojaei F, Levac K, Cerdan C, et al. (2004) Endothelial and hematopoietic cell fate of human embryonic stem cells originates from primitive endothelium with hemangioblastic properties. Immunity 21: 31–41.
32. Wang L, Menendez P, Shojaei F, Li L, Mazurier F, et al. (2005) Generation of hematopoietic repopulating cells from human embryonic stem cells independent of ectopic HOXB4 expression. J Exp Med 201: 1603–1614.
33. Nostro MC, Cheng X, Keller GM, Gadue P (2008) Wnt, activin, and BMP signaling regulate distinct stages in the developmental pathway from embryonic stem cells to blood. Cell Stem Cell 2: 60–71.
34. Gadue P, Huber TL, Paddison PJ, Keller GM (2006) Wnt and TGF-beta signaling are required for the induction of an in vitro model of primitive streak formation using embryonic stem cells. Proc Natl Acad Sci U S A 103: 16806–16811.
35. Kennedy M, D'Souza SL, Lynch-Kattman M, Schwantz S, Keller G (2007) Development of the hemangioblast defines the onset of hematopoiesis in human ES cell differentiation cultures. Blood 109: 2679–2687.
36. Martin R, Lahlil R, Damert A, Miquerol L, Nagy A, et al. (2004) SCL interacts with VEGF to suppress apoptosis at the onset of hematopoiesis. Development 131: 693–702.
37. Grigoriadis AE, Kennedy M, Bozec A, Brunton F, Stenbeck G, et al. (2010) Directed differentiation of hematopoietic precursors and functional osteoclasts from human ES and iPS cells. Blood 115: 2769–2776.
38. Takahashi K, Tanabe K, Ohnuki M, Narita M, Ichisaka T, et al. (2007) Induction of pluripotent stem cells from adult human fibroblasts by defined factors. Cell 131: 861–872.
39. Suemori H, Yasuchika K, Hasegawa K, Fujioka T, Tsuneyoshi N, et al. (2006) Efficient establishment of human embryonic stem cell lines and long-term maintenance with stable karyotype by enzymatic bulk passage. Biochem Biophys Res Commun 345: 926–932.
40. Suwabe N, Takahashi S, Nakano T, Yamamoto M (1998) GATA-1 regulates growth and differentiation of definitive erythroid lineage cells during in vitro ES cell differentiation. Blood 92: 4108–4118.
41. Nakahata T, Ogawa M (1982) Hemopoietic colony-forming cells in umbilical cord blood with extensive capability to generate mono- and multipotential hemopoietic progenitors. J Clin Invest 70: 1324–1328.
42. Nakahata T, Ogawa M (1982) Identification in culture of a class of hemopoietic colony-forming units with extensive capability to self-renew and generate multipotential hemopoietic colonies. Proc Natl Acad Sci U S A 79: 3843–3847.
43. Nakahata T, Spicer SS, Ogawa M (1982) Clonal origin of human erythro-eosinophilic colonies in culture. Blood 59: 857–864.
44. Uchida T, Kanno T, Hosaka S (1985) Direct measurement of phagosomal reactive oxygen by luminol-binding microspheres. J Immunol Methods 77: 55–61.
45. Ma F, Ebihara Y, Umeda K, Sakai H, Hanada S, et al. (2008) Generation of functional erythrocytes from human embryonic stem cell-derived definitive hematopoiesis. Proc Natl Acad Sci U S A 105: 13087–13092.
46. Fujimi A, Matsunaga T, Kobune M, Kawano Y, Nagaya T, et al. (2008) Ex vivo large-scale generation of human red blood cells from cord blood CD34+ cells by co-culturing with macrophages. Int J Hematol 87: 339–350.
47. Yamaguchi TP, Dumont DJ, Conlon RA, Breitman ML, Rossant J (1993) flk-1, an flt-related receptor tyrosine kinase is an early marker for endothelial cell precursors. Development 118: 489–498.
48. Asahara T, Murohara T, Sullivan A, Silver M, van der Zee R, et al. (1997) Isolation of putative progenitor endothelial cells for angiogenesis. Science 275: 964–967.
49. Kennedy M, Firpo M, Choi K, Wall C, Robertson S, et al. (1997) A common precursor for primitive erythropoiesis and definitive haematopoiesis. Nature 386: 488–493.
50. Grigoriadis AE, Kennedy M, Bozec A, Brunton F, Stenbeck G, et al. (2010) Directed differentiation of hematopoietic precursors and functional osteoclasts from human ES and iPS cells. Blood 115: 2769–2776.
51. Kim K, Doi A, Wen B, Ng K, Zhao R, et al. (2010) Epigenetic memory in induced pluripotent stem cells. Nature 467: 285–290.
52. Osafune K, Caron L, Borowiak M, Martinez RJ, Fitz-Gerald CS, et al. (2008) Marked differences in differentiation propensity among human embryonic stem cell lines. Nat Biotechnol 26: 313–315.
53. Ji H, Ehrlich LI, Seita J, Murakami P, Doi A, et al. (2010) Comprehensive methylome map of lineage commitment from haematopoietic progenitors. Nature 467: 338–342.
54. Kyba M, Perlingeiro RC, Daley GQ (2002) HoxB4 confers definitive lymphoid-myeloid engraftment potential on embryonic stem cell and yolk sac hematopoietic progenitors. Cell 109: 29–37.
55. Raaijmakers MH, Mukherjee S, Guo S, Zhang S, Kobayashi T, et al. (2010) Bone progenitor dysfunction induces myelodysplasia and secondary leukaemia. Nature 464: 852–857.

ARTHRITIS & RHEUMATISM
Vol. 63, No. 11, November 2011, pp 3625–3632
DOI 10.1002/art.30512

High Incidence of *NLRP3* Somatic Mosaicism in Patients With Chronic Infantile Neurologic, Cutaneous, Articular Syndrome

Results of an International Multicenter Collaborative Study

Naoko Tanaka,[1] Kazushi Izawa,[1] Megumu K. Saito,[2] Mio Sakuma,[3] Koichi Oshima,[4] Osamu Ohara,[4] Ryuta Nishikomori,[1] Takeshi Morimoto,[3] Naotomo Kambe,[5] Raphaela Goldbach-Mansky,[6] Ivona Aksentijevich,[6] Geneviève de Saint Basile,[7] Bénédicte Neven,[8] Mariëlle van Gijn,[9] Joost Frenkel,[9] Juan I. Aróstegui,[10] Jordi Yagüe,[10] Rosa Merino,[11] Mercedes Ibañez,[12] Alessandra Pontillo,[13] Hidetoshi Takada,[14] Tomoyuki Imagawa,[15] Tomoki Kawai,[1] Takahiro Yasumi,[1] Tatsutoshi Nakahata,[2] and Toshio Heike[1]

Objective. **Chronic infantile neurologic, cutaneous, articular (CINCA) syndrome, also known as neonatal-onset multisystem inflammatory disease (NOMID), is a dominantly inherited systemic autoinflammatory disease. Although heterozygous germline gain-of-function *NLRP3* mutations are a known cause of this disease, conventional genetic analyses fail to detect disease-causing mutations in ~40% of patients. Since somatic *NLRP3* mosaicism has been detected in several mutation-negative NOMID/CINCA syndrome patients, we undertook this study to determine the precise contribution of somatic *NLRP3* mosaicism to the etiology of NOMID/CINCA syndrome.**

Methods. **An international case–control study was performed to detect somatic *NLRP3* mosaicism in NOMID/CINCA syndrome patients who had shown no mutation during conventional sequencing. Subcloning and sequencing of *NLRP3* was performed in these mutation-negative NOMID/CINCA syndrome patients and their healthy relatives. Clinical features were analyzed to identify potential genotype–phenotype associations.**

Results. **Somatic *NLRP3* mosaicism was identified in 18 of the 26 patients (69.2%). Estimates of the level of mosaicism ranged from 4.2% to 35.8% (mean ± SD 12.1 ± 7.9%). Mosaicism was not detected in any of the 19 healthy relatives (18 of 26 patients versus 0 of 19**

Supported by Mitsubishi Pharma Research Foundation, the Japanese Ministry of Education, Science, Sports, and Culture, and the Japanese Ministry of Health, Labor, and Welfare.

[1]Naoko Tanaka, MD, Kazushi Izawa, MD, Ryuta Nishikomori, MD, PhD, Tomoki Kawai, MD, Takahiro Yasumi, MD, PhD, Toshio Heike, MD, PhD: Kyoto University Graduate School of Medicine, Kyoto, Japan; [2]Megumu K. Saito, MD, PhD, Tatsutoshi Nakahata, MD, PhD: Center for iPS Cell Research and Application, Kyoto, Japan; [3]Mio Sakuma, MD, PhD, Takeshi Morimoto, MD, PhD: Kyoto University, Kyoto, Japan; [4]Koichi Oshima, MD, Osamu Ohara, PhD: RIKEN Yokohama Institute, Yokohama, Kanagawa, and Kazusa DNA Research Institute, Kisarazu, Chiba, Japan; [5]Naotomo Kambe, MD, PhD: Chiba University Graduate School of Medicine, Chiba, Japan; [6]Raphaela Goldbach-Mansky, MD, Ivona Aksentijevich, MD: National Institute of Arthritis and Musculoskeletal and Skin Diseases, NIH, Bethesda, Maryland; [7]Geneviève de Saint Basile, MD, PhD: Paris Descartes University and INSERM U 768, Paris, France; [8]Bénédicte Neven, MD: Necker Hospital for Sick Children, AP-HP, Paris, France; [9]Mariëlle van Gijn, PhD, Joost Frenkel, MD, PhD: University Medical Centre Utrecht, Utrecht, The Netherlands; [10]Juan I. Aróstegui, MD, PhD, Jordi Yagüe, MD, PhD: Hospital Clínic, Barcelona, Spain; [11]Rosa Merino, MD, PhD: Hospital La Paz, Madrid, Spain; [12]Mercedes Ibañez, MD: Hospital Niño Jesús, Madrid, Spain; [13]Alessandra Pontillo, MD, PhD: IRCCS Burlo Garofalo, Trieste, Italy; [14]Hidetoshi Takada, MD, PhD: Kyushu University Graduate School of Medical Sciences, Fukuoka, Japan; [15]Tomoyuki Imagawa, MD, PhD:Yokohama City University School of Medicine, Yokohama, Kanagawa, Japan.

Drs. Tanaka and Izawa contributed equally to this work.

Dr. Goldbach-Mansky has served as an expert witness on behalf of Biovitrum, Novartis, and Regeneron.

Address correspondence to Osamu Ohara, PhD, Department of Human Genome Research, Kazusa DNA Research Institute, 2-6-7 Kazusakamatari Kisarazu, Chiba 292-0818, Japan (e-mail: ohara@kazusa.or.jp); or to Ryuta Nishikomori, MD, PhD, Department of Pediatrics, Kyoto University Graduate School of Medicine, 54 Shogoin Sakyo, Kyoto 606-8507, Japan (e-mail: rnishiko@kuhp.kyoto-u.ac.jp).

Submitted for publication March 10, 2011; accepted in revised form June 16, 2011.

relatives; $P < 0.0001$). In vitro functional assays indicated that the detected somatic *NLRP3* mutations had disease-causing functional effects. No differences in *NLRP3* mosaicism were detected between different cell lineages. Among nondescript clinical features, a lower incidence of mental retardation was noted in patients with somatic mosaicism. Genotype-matched comparison confirmed that patients with somatic *NLRP3* mosaicism presented with milder neurologic symptoms.

Conclusion. **Somatic *NLRP3* mutations were identified in 69.2% of patients with mutation-negative NOMID/CINCA syndrome. This indicates that somatic *NLRP3* mosaicism is a major cause of NOMID/CINCA syndrome.**

Chronic infantile neurologic, cutaneous, articular (CINCA) syndrome (MIM no. #607715), also known as neonatal-onset multisystem inflammatory disease (NOMID), is a dominantly-inherited autoinflammatory disease that is characterized by neonatal onset and the triad of urticarial-like skin rash, neurologic manifestations, and arthritis/arthropathy. Patients often experience recurrent fever and systemic inflammation. NOMID/CINCA syndrome is the most severe clinical phenotype of the cryopyrin-associated periodic syndromes (CAPS) that also include the 2 less severe but phenotypically similar syndromes familial cold autoinflammatory syndrome (FCAS; MIM no. #120100) and Muckle-Wells syndrome (MIM no. #191900). CAPS are caused by mutations in the *NLRP3* gene, which is a member of the nucleotide-binding oligomerization domain–like receptor (NLR) family of the innate immune system (1,2).

NLRP3 is an intracellular "sensor" of danger signals arising from cellular insults, such as infection, tissue damage, and metabolic deregulation, and it has been highly conserved throughout evolution. NLRP3 associates with ASC and procaspase 1 to constitute a large multiprotein complex termed the NLRP3 inflammasome. When activated, the NLRP3 inflammasome converts the biologically inactive procaspase 1 into active caspase 1. Caspase 1 produces the cytokines interleukin-1β (IL-1β) and IL-18, which are mainly involved in the inflammatory response (3). Available research suggests that mutated *NLRP3* induces autoactivation of the NLRP3 inflammasome in CAPS patients, resulting in an uncontrolled overproduction of IL-1β.

Most CAPS patients carry heterozygous germline missense mutations in the *NLRP3* coding region ("mutation-positive" patients) (4,5). More than 80 different disease-causing mutations have been reported to date (6). However, ~40% of clinically diagnosed NOMID/CINCA syndrome patients show no heterozygous germline *NLRP3* mutation during conventional Sanger-sequencing-based genetic analyses ("mutation-negative" patients). Comparisons of NOMID/CINCA syndrome patients with and without heterozygous germline *NLRP3* mutations have revealed no differences in clinical features or response to treatment (4,7).

In a previous study, we identified a high incidence of somatic *NLRP3* mosaicism in "mutation-negative" NOMID/CINCA syndrome patients in Japan (8). We therefore hypothesized that somatic *NLRP3* mosaicism may be implicated in the etiology of the disorder, although its precise contribution remains unclear. The aim of the present study was to evaluate both the frequency of *NLRP3* somatic mosaicism in NOMID/CINCA syndrome patients and the association between somatic mosaicism and clinical phenotype using an international cohort of mutation-negative NOMID/CINCA syndrome patients.

PATIENTS AND METHODS

Study design and participants. International collaborators were contacted to identify mutation-negative NOMID/CINCA syndrome cases. A total of 20 DNA samples were received from 4 centers: France (n = 6), The Netherlands (n = 4), Spain (n = 3), and the US (n = 7). DNA samples had been extracted from peripheral blood mononuclear cells or whole blood. All 20 samples had been subjected to conventional sequencing, and no *NLRP3* mutations had been identified. In each case, the accuracy of the clinical diagnosis had been confirmed according to the diagnostic criteria (7). The 6 previously reported Japanese cases and 1 Spanish case with *NLRP3* somatic mosaicism were also included (8,9). DNA samples were also collected from 19 healthy relatives of 8 patients (8 from France, 5 from Japan, 2 from Spain, and 4 from the US) to evaluate the causality of somatic *NLRP3* mosaicism in a case–control manner, since the clinical features may be modified by genetic and environmental factors.

Written informed consent for *NLRP3* gene analysis was obtained from all patients and controls. The study was approved by the Institutional Review Board of the Kyoto University Graduate School of Medicine and was conducted in accordance with the Declaration of Helsinki.

Data collection. *Demographic and clinical data.* The clinicians responsible for each mutation-negative NOMID/CINCA syndrome patient completed a questionnaire to document characteristics such as age, sex, race, symptoms, clinical findings, clinical course, and prognosis. No clinical data were obtained from the healthy controls.

Investigation of NLRP3 gene mosaicism. Disease-causing mutations in NOMID/CINCA syndrome patients have

only been reported in exons 3, 4, and 6 of *NLRP3* (6). Thus, the present sequencing was focused on a search for somatic mosaicism of these 3 exons and their flanking intronic regions. After amplifying these genomic regions with the proofreading polymerase chain reaction (PCR) enzyme KOD-Plus polymerase (Toyobo) and dA addition with an LA *Taq* polymerase (Takara Bio), the amplicons were subcloned into pCR2.1-TOPO vector (Invitrogen). Ninety-six clones were selected at random for each amplicon. The subcloned amplicons were retrieved by PCR with LA *Taq* polymerase. They were then treated with ExoSAP-IT (USB) and proteinase K (Promega) prior to direct sequencing. The cloned exons were sequenced at the Kazusa DNA Research Institute using a BigDye Terminator kit (version 3.1) and an ABI 3730 DNA sequencer (Life Technologies). Mosaicism was indicated by the detection of >2 subclones carrying the same base variation at the same position in 96 clones.

To purify leukocyte subpopulations, freshly drawn whole blood was separated using sequential dextran and Ficoll-Hypaque density-gradient centrifugation methods. Cell sorting to select T cells, B cells, and monocytes was performed with an AutoMACS Pro Separator (Miltenyi Biotec) or a FACSVantage System (BD Biosciences), as described elsewhere (8,9). The purity of each cell lineage was >90%. The level of mosaicism was determined by sequencing each source of genomic DNA from 80 clones.

Plasmids and cell lines. To determine whether the identified NLRP3 mutants cause disease, experiments for assessing 2 pathologic functions were performed as described elsewhere (8). Briefly, ASC-dependent NF-κB activation was performed by a dual-luciferase reporter assay in HEK 293FT cells transfected with NLRP3 mutants. Transfection-induced cell death in the human monocytic cell line THP-1 was performed by transfecting green fluorescent protein–fused mutant NLRP3 into THP-1 cells and then measuring the dead cells with 7-aminoactinomycin D.

Statistical analysis. The study was designed to detect mosaicism at a 5% allele frequency with >95% possibility. To satisfy this condition, it was necessary to sequence at least 93 clones per patient. The following calculation was used to estimate the number of clones that had to be sequenced: $P = 1 - (1 - 0.05)^n - n(0.05)(1 - 0.05)^{n-1}$ ($n = 93$, $P = 0.956$). The study was designed to analyze 96 PCR-fragment clones from each patient. The error rate of the PCR reactions was estimated using a proofreading KOD-Plus enzyme. We analyzed a plasmid vector carrying a normal *NLRP3* exon 3, in which 2 distinct errors were detected by sequencing 91 clones. The calculated error rate for this result was 1/87,451 (2/[1,922 bp × 91 clones]). Thus, the probability was negligible that the same errors would be detected more than twice in 96 clones from 1 patient.

To calculate the sample size, we calculated the prevalence of somatic mosaicism among mutation-negative NOMID/CINCA syndrome patients. Eight cases of somatic mosaicism were identified among 15 mutation-negative NOMID/CINCA syndrome patients who were subsequently analyzed by the subcloning method described above. It was assumed that the maximum number of possible somatic mosaicism cases among family controls was 1. On the basis of these data and this assumption, it was calculated that 19 controls were required to ensure a 2-sided alpha level of 0.05 and a power of 0.8.

Continuous variables are presented as the mean ± SD or as the median and interquartile range. Categorical variables are presented as numbers and ratios (with percentages). To compare clinical data between patients with and patients without mosaicism, the Wilcoxon rank sum test was used for continuous variables and Fisher's exact test was used for categorical variables. Fisher's exact test was used to compare the difference in mosaicism ratio between cases and controls. The chi-square test was used to compare the difference in the level of mosaicism between different sources of genomic DNA from each patient.

Table 1. Somatic mosaicism among mutation-negative NOMID/CINCA syndrome patients*

Country, patient	Sequence variant	Protein variant	Mosaicism, %
France			
F1	1298C>T	T433I	5.2
F2	907G>C	D303H	4.2
F3	1315G>C	A439P	21.9
F4	1216A>G	M406V	9.2
F5	1698C>A	F566L	11.5
F6	None	–	–
Japan			
J1	1709A>G	Y570C	12.2
J2	790C>T	L264F	4.3
J3	919G>A	G307S	10.7
J4	1699G>A	E567K	6.5
J5	907G>C	D303H	11.9
J6	None	–	–
Spain			
S1	920G>T	G307V	9.6
S2	907G>C	D303H	19.1
S3	None	–	–
S4	None	–	–
US			
A1	1065A>T	K355N	18.8
A2	1698C>A	F566L	14.6
A3	1704G>C	K568N	9.4
A4	2263G>A	G755R	35.8
A5	None	–	–
A6	None	–	–
The Netherlands			
N1	1699G>A	E567K	6.3
N2	2263G>A	G755R	6.3
N3	None	–	–
N4	None	–	–

* *NLRP3* mosaicism was detected in 18 of 26 patients (69.2%) with neonatal-onset multisystem inflammatory disease (NOMID)/chronic infantile neurologic, cutaneous, articular syndrome (CINCA syndrome). When samples from 19 healthy relatives of these patients were investigated, no somatic mosaicism was detected. The *P* value from the comparison of the cases and the controls (18 of 26 versus 0 of 19) was statistically significant ($P < 0.0001$).

RESULTS

Somatic *NLRP3* mosaicism in mutation-negative NOMID/CINCA syndrome patients. A heterozygous germline *NLRP3* mutation was detected in 1 of the 27 samples, and this was therefore excluded from the analyses. For each patient, 96 clones were selected at random for each amplicon. These were then sequenced. *NLRP3* mosaicism was detected in 18 of 26 patients (69.2%), and the level of allelic mosaicism ranged from 4.2% to 35.8% (mean ± SD 12.1 ± 7.9%; median 10.2%) (Table 1). Seven of the detected *NLRP3* mutations were novel (p.G307S, p.K355N, p.M406V, p.T433I, p.F566L, p.E567K, and p.K568N). The remaining mutations have been reported previously in NOMID/CINCA syndrome patients as disease-causing heterozygous germline mutations (p.L264F, p.D303H, p.G307V, p.A439P, p.Y570C, and p.G755R). Each of the 3 *NLRP3* mutations, p.F566L, p.E567K, and p.G755R, was detected in 2 unrelated patients. *NLRP3* mutation p.D303H was detected in 3 unrelated patients.

Analyses in family controls. To validate the clinical relevance of the *NLRP3* mosaicism identified in mutation-negative NOMID/CINCA syndrome patients, samples from 19 healthy relatives were investigated. No somatic mosaicism was detected in any of these samples. The *P* value from the comparison of cases and controls (18 of 26 versus 0 of 19) was statistically significant ($P < 0.0001$).

Functional effects of the identified somatic *NLRP3* mutations. Since disease-causing heterozygous germline mutations in *NLRP3* have been implicated in necrosis-like programmed cell death and ASC-dependent NF-κB activation (8), experiments were performed to determine whether the mutations identified in patients with somatic mosaicism showed the same effects. All of the identified mutations induced both THP-1 cell death (Figure 1A) and ASC-dependent NF-κB activation (Figure 1B). The in vitro effects of these novel mutations were similar to or even more pronounced than those of previously reported *NLRP3* mutations. This strongly suggests that all mutations showing somatic mosaicism have pathogenic effects, including the novel mutations identified in the present study.

Mutation frequency of *NLRP3* among various cell lineages and 1 tissue type. To explore the origin of the *NLRP3* mosaicism, mutational frequency was evaluated in various cell lineages and 1 tissue type from 4 Japanese patients with *NLRP3* somatic mosaicism. In each patient, the same mutations were found in all of the cell lineages investigated (neutrophils, monocytes, T cells, B cells) and in the buccal mucosa tissue, and no significant difference in mutation frequency was observed between these sources (Table 2).

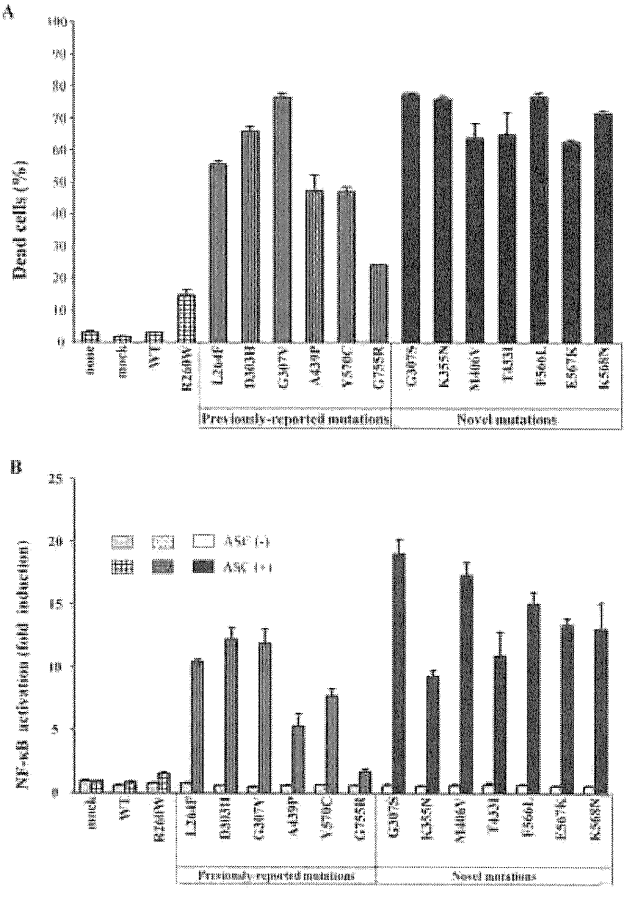

Figure 1. In vitro functional assessment of the identified *NLRP3* mosaicism mutations. **A,** Necrotic cell death of THP-1 cells induced by the identified somatic *NLRP3* mosaicism mutations. Green fluorescent protein (GFP)–fused mutant NLRP3 was transfected into THP-1 cells. The percentage of dead cells (7-aminoactinomycin D positive) among GFP-positive cells is shown. Values are the mean ± SD of triplicate experiments, and data are representative of 2 independent experiments. None = nothing transfected; mock = vector without NLRP3; WT = wild-type NLRP3; R260W = NLRP3 with p.R260W (frequent mutations in patients with cryopyrin-associated periodic syndromes). **B,** ASC-dependent NF-κB activation induced by the identified somatic *NLRP3* mosaicism mutations. HEK 293FT cells were cotransfected with WT or mutant NLRP3 in the presence or absence of ASC. The induction of NF-κB is shown as the fold change compared with cells that were transfected with a control vector without ASC (set at 1). Values are the mean ± SD of triplicate experiments, and data are representative of 2 independent experiments.

Table 2. Distribution and quantification of *NLRP3* mutations among sources of genomic DNA (4 cell lineages and 1 tissue type)*

Patient	Sequence variant	Protein variant	Mosaicism, %				
			Neutrophils	Monocytes	T cells	B cells	Buccal mucosa
J1	1709A>G	Y570C	12.6	9.8	8.0	9.5	8.3
J3	919G>A	G307S	9.1	10.8	6.9	10.6	9.0
J4	1699G>A	E567K	3.5	2.3	3.7	3.4	2.2
J5	907G>C	D303H	14.4	8.7	7.7	8.5	13.5

* No significant differences in the level of mosaicism were observed among the sources of genomic DNA.

Phenotype–genotype analysis. Given the previously reported genotype–phenotype association between the *NLRP3* gene and CAPS, the clinical characteristics of NOMID/CINCA syndrome patients with somatic *NLRP3* mutations were compared with those of patients from previous reports who had the same *NLRP3* mutations but with heterozygous germline status (1,4,10–13) (Figure 2) (further information is available at http://web16.kazusa.or.jp/download/). All of the patients in these 2 groups had an early onset of the disease, fever, and urticarial rash. The presence of arthritis, bony overgrowth, contractures, hearing loss, and seizure varied in each group of patients, and no significant difference was detected. However, whereas most patients with heterozygous germline *NLRP3* mutations presented with mental retardation, this was not the case for patients with somatic *NLRP3* mosaicism. A comparison was also made between the clinical data from patients with somatic *NLRP3* mosaicism and the data from patients with neither germline nor somatic *NLRP3* mutations. Again, a lower incidence of mental retardation was observed in patients with somatic *NLRP3* mosaicism

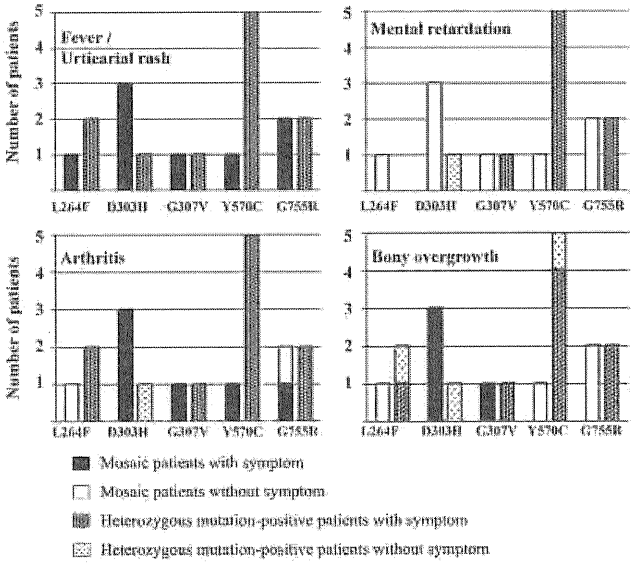

Figure 2. Comparison of the clinical profiles of patients carrying somatic *NLRP3* mutations and patients carrying the same mutation, but with germline status. Clinical profiles of patients with mosaicism and those of patients with heterozygous germline mutations are compared for each protein variant (L264F, D303H, G307V, Y570C, and G755R). The data on 4 typical clinical symptoms are shown. Total numbers of patients with mosaicism and total numbers of patients with heterozygous mutation examined are shown as a bar for each protein variant. Each bar is stratified according to the presence or absence of the symptom. For the protein variant L264F, no data on mental retardation were available for the patient with a heterozygous germline mutation.

Table 3. Clinical profiles of patients with somatic *NLRP3* mosaicism and patients with neither germline nor somatic *NLRP3* mutations*

	Patients with somatic *NLRP3* mosaicism (n = 18)	Patients with neither germline nor somatic *NLRP3* mutations (n = 8)
Age, median (IQR) years	12 (1–30)	10 (3–21)
No. of men/women	10/8	3/5
Age at onset, median (IQR) months	0 (0–24)	0.5 (0–33)
Fever	17/17	7/7
Urticarial rash	14/14	8/8
Mental retardation	4/17	6/8
Meningitis	13/17	5/8
Seizures	2/18	1/7
Hearing loss	10/18	2/7
Arthritis	14/17	7/8
Bony overgrowth	12/17	6/7
Contractures	7/17	4/7
Walking disability	8/18	3/7
Biologic therapy	10/15	3/8

* Except where indicated otherwise, values are the number with the feature/the total number of patients assessed. A lower incidence of mental retardation was observed in patients with somatic *NLRP3* mosaicism ($P = 0.03$). No other significant differences were detected between the groups. IQR = interquartile range.

(P = 0.03). No other significant differences were detected (Table 3) (further information is available at http://web16.kazusa.or.jp/download/).

DISCUSSION

The present international multicenter study investigated 26 NOMID/CINCA syndrome patients who were mutation negative according to conventional sequencing along with 19 family controls to determine whether low-level mosaicism is a disease-causing genetic mechanism. Following our first report of low-level somatic mosaicism in a NOMID/CINCA syndrome patient (14), we reported a new method of detecting low-level *NLRP3* mosaicism, in which lipopolysaccharide (LPS) induced cell death specifically in *NLRP3* mutation–positive monocytes (8). However, this method requires fresh live monocytes, special equipment such as a cell sorter, and experience in its use due to the rapid time course of LPS-induced necrotic monocytic death. For these reasons, application of this method was not feasible in an international collaborative study. We therefore opted to use genomic DNA, since it is easier to handle and can be stored and shipped. Based on our previous study in Japanese patients showing that the frequency of mutant alleles could be <5%, we designed a subcloning and Sanger-sequencing strategy that could detect this very low allelic mutation frequency.

Presuming that the present cohort is representative of the 40% of NOMID/CINCA syndrome patients who are mutation negative according to conventional sequencing, the results suggest that ~28% of all NOMID/CINCA syndrome patients may carry somatic *NLRP3* mosaicism. CAPS patients present with a continuous spectrum of symptoms, and a degree of genotypic overlap is observed between disease subtypes. Although the present study focused on the most severe NOMID/CINCA syndrome phenotype, it is possible that somatic *NLRP3* mosaicism may also occur in milder forms of CAPS. The presence of somatic mosaicism should also be investigated in patients with other dominantly inherited autoinflammatory diseases caused by gain-of-function mutations and who are mutation negative according to conventional sequencing.

Among the 18 patients with somatic *NLRP3* mosaicism, we found 6 mutations that have previously been identified in NOMID/CINCA syndrome patients as heterozygous germline mutations. We also identified 7 novel mutations, which were confirmed as being functionally active and presumably pathogenic. Functional in vitro assays showed that these novel mutations had greater disease-causing capacity than the previously described mutations. This suggests that the novel mutations may be deleterious and unrecognized if inherited as heterozygous germline mutations.

The present study also addressed the important question of how somatic *NLRP3* mosaicism modifies clinical presentation. Although no statistically significant differences in age at disease onset, skin symptoms, joint involvement, or response to IL-1 blockade were detected, milder neurologic involvement was observed in patients with somatic mosaicism. Comparisons with NOMID/CINCA syndrome patients carrying the same *NLRP3* mutations but with heterozygous germline status made this tendency more prominent. Although the level of somatic mosaicism in blood leukocytes was relatively low, it remains unclear how these low-level mutations influence clinical presentation, including disease severity. One interesting hypothesis is that the difference in the severity of neurologic manifestations is a function of the level of mosaicism. For ethical and technical reasons, it was not possible to evaluate the level of mosaicism in central nervous system (CNS) cells or glial cells in the present study, and this therefore awaits investigation in future studies.

The mechanism through which *NLRP3* somatic mosaicism occurs also requires elucidation. The present study demonstrated that similar proportions of neutrophils, T cells, B cells, monocytes, and buccal cells carried the mutated allele. Therefore, the mutation leading to mosaicism must have arisen before the pluripotent stem cells committed to hematopoietic progenitor stem cells or ectoderm-derived nonhematopoietic cells. Several mechanisms for mosaicism have been proposed, including chimerism due to cell fusion with an aborted dizygotic twin and a mutational event during early embryogenesis (15). The latter mechanism is more likely in the present cohort, since mosaicism at similar frequency was detected in several cell types. To verify the hypothesis of a mutational event during embryogenesis, and to determine the point at which this occurred, it would be helpful to analyze other tissues. However, obtaining such tissues from patients may be ethically problematic.

Approximately 12% of the patients in the present cohort carried neither germline nor somatic *NLRP3* mutations and may therefore be considered to be genuinely mutation negative. However, it is possible that these patients have *NLRP3* mutations that have been overlooked. A recent report described a mutation in the 5′-untranslated region of *NLRP3* in a patient with FCAS

(16), although it remains unclear how this noncoding mutation causes disease. Another possibility is that an extremely low frequency of NLRP3 mosaicism may have been missed. The subcloning and Sanger-sequencing strategy used in this study set the detection limit of mosaicism at 5%. Considering the range of *NLRP3* mosaicism detected (4.2–35.8%), the median (10.2%), and the identification of 2 patients with <5% mosaicism, it is indeed likely that patients with an even lower level of *NLRP3* mosaicism may have been overlooked. Recent advances in next-generation DNA sequencing technology may resolve this technical problem, although the associated error rate could be problematic. Another possibility is that *NLRP3* mutations were present in uninvestigated cell lineages, such as those from CNS tissue, bone tissue, or skin. Future studies of NOMID/CINCA syndrome should investigate these tissues while searching for mutations in other genes.

In conclusion, the present study has clearly demonstrated that a significant proportion of NOMID/CINCA syndrome patients who were mutation negative according to conventional sequencing carried somatic *NLRP3* mutations with a variable degree of mosaicism. Clinicians should therefore consider somatic mosaicism as a possible cause of disease in mutation-negative NOMID/CINCA syndrome patients and implement appropriate therapy. The early diagnosis of NOMID/CINCA syndrome and prompt initiation of therapy would improve clinical outcome. Further goals in this research field are the refinement of genetic screening and the verification of the functional consequences of all detected somatic mutations. Systematic screening for somatic mosaicism will provide new insights into the etiology of human disease.

ACKNOWLEDGMENTS

We thank all patients and their relatives for participating in the study. We are grateful to Yuki Takaoka at the Department of Pediatrics, Kyoto University Graduate School of Medicine and Seiko Watanabe at the Department of Human Genome Research, Kazusa DNA Research Institute for their technical assistance.

AUTHOR CONTRIBUTIONS

All authors were involved in drafting the article or revising it critically for important intellectual content, and all authors approved the final version to be published. Drs. Ohara and Nishikomori had full access to all of the data in the study and take responsibility for the integrity of the data and the accuracy of the data analysis.

Study conception and design. Saito, Ohara, Nishikomori, Kambe.

Acquisition of data. Tanaka, Izawa, Saito, Oshima, Ohara, Nishikomori, Goldbach-Mansky, Aksentijevich, de Saint Basile, Neven, van Gijn, Frenkel, Aróstegui, Yagüe, Merino, Ibañez, Pontillo, Takada, Imagawa.

Analysis and interpretation of data. Sakuma, Morimoto, Kawai, Yasumi, Nakahata, Heike.

ROLE OF THE STUDY SPONSOR

Mitsubishi Pharma Research Foundation supported the data collection for this study, approved the contents of the manuscript, and agreed to submit the manuscript for publication.

REFERENCES

1. Neven B, Callebaut I, Prieur AM, Feldmann J, Bodemer C, Lepore L, et al. Molecular basis of the spectral expression of CIAS1 mutations associated with phagocytic cell-mediated autoinflammatory disorders CINCA/NOMID, MWS, and FCU. Blood 2004;103:2809–15.
2. Stojanov S, Kastner DL. Familial autoinflammatory diseases: genetics, pathogenesis and treatment. Curr Opin Rheumatol 2005; 17:586–99.
3. Schroder K, Zhou R, Tschopp J. The NLRP3 inflammasome: a sensor for metabolic danger? Science 2010;327:296–300.
4. Aksentijevich I, Nowak M, Mallah M, Chae JJ, Watford WT, Hofmann SR, et al. De novo CIAS1 mutations, cytokine activation, and evidence for genetic heterogeneity in patients with neonatal-onset multisystem inflammatory disease (NOMID): a new member of the expanding family of pyrin-associated autoinflammatory diseases. Arthritis Rheum 2002;46:3340–8.
5. Hoffman HM, Mueller JL, Broide DH, Wanderer AA, Kolodner RD. Mutation of a new gene encoding a putative pyrin-like protein causes familial cold autoinflammatory syndrome and Muckle-Wells syndrome. Nat Genet 2001;29:301–5.
6. Milhavet F, Cuisset L, Hoffman HM, Slim R, El-Shanti H, Aksentijevich I, et al. The Infevers autoinflammatory mutation online registry: update with new genes and functions. Hum Mutat 2008;29:803–8.
7. Goldbach-Mansky R, Dailey NJ, Canna SW, Gelabert A, Jones J, Rubin BI, et al. Neonatal-onset multisystem inflammatory disease responsive to interleukin-1β inhibition. N Engl J Med 2006;355: 581–92.
8. Saito M, Nishikomori R, Kambe N, Fujisawa A, Tanizaki H, Takeichi K, et al. Disease-associated CIAS1 mutations induce monocyte death, revealing low-level mosaicism in mutation-negative cryopyrin-associated periodic syndrome patients. Blood 2008;111:2132–41.
9. Arostegui JI, Lopez Saldana MD, Pascal M, Clemente D, Aymerich M, Balaguer F, et al. A somatic NLRP3 mutation as a cause of a sporadic case of chronic infantile neurologic, cutaneous, articular syndrome/neonatal-onset multisystem inflammatory disease: novel evidence of the role of low-level mosaicism as the pathophysiologic mechanism underlying Mendelian inherited diseases. Arthritis Rheum 2010;62:1158–66.
10. Rosen-Wolff A, Quietzsch J, Schroder H, Lehmann R, Gahr M, Roesler J. Two German CINCA (NOMID) patients with different clinical severity and response to anti-inflammatory treatment. Eur J Haematol 2003;71:215–9.
11. Aksentijevich I, Putnam CD, Remmers EF, Mueller JL, Le J, Kolodner RD, et al. The clinical continuum of cryopyrinopathies: novel CIAS1 mutations in North American patients and a new cryopyrin model. Arthritis Rheum 2007;56:1273–85.
12. Matsubayashi T, Sugiura H, Arai T, Oh-Ishi T, Inamo Y. Anakinra